ENGINEERING RESEARCH

BULLETIN NO. 107

DATA ANALYSIS AND CORRELATION WITH DIGITAL COMPUTERS-- NONDESTRUCTIVE TESTING

(FINAL REPORT)

BY

LAWRENCE MANN, JR. AND MYRON H. YOUNG

DIVISION OF ENGINEERING RESEARCH

LOUISIANA STATE UNIVERSITY

Reproduced by
NATIONAL TECHNICAL
INFORMATION SERVICE
Springfield, Va. 22151

BATON ROUGE, LOUISIANA 70803

1971

DATA ANALYSIS AND CORRELATION

WITH DIGITAL COMPUTERS--NONDESTRUCTIVE TESTING

by

Lawrence Mann, Jr., Professor
and
Myron H. Young, Associate Professor

Final Report

July 1, 1970 to August 31, 1971

Sponsored by

Advanced Research Projects Agency
ARPA Order No. 1246

Contract No. DAAA 25-69-C0079

Frankford Arsenal
Philadelphia, Pennsylvania 19137

Prepared by

Industrial Engineering Department
Louisiana State University
Baton Rouge, Louisiana 70803

FOREWARD

This Final Report was prepared by the Industrial Engineering Division, Louisiana State University, Baton Rouge, Louisiana, 70803, under contract number DAAA 25-69-C0079 and covers the work accomplished between September 12, 1968 and August 31, 1971. This is the Final Report for Data Analysis and Correlation with Digital Computers--Nondestructive Testing. Phases I and II were conducted between September 1968 and June 1970.

The program was sponsored by the Advanced Research Projects Agency of the Department of Defense ARPA Order 1246. The program was under the direction of Mr. Eugene Roffman of the Frankford Arsenal, Philadelphia, Pennsylvania, 19137. The contract was administered by the Office of Naval Research Resident Representative, University of Texas, Room 2507-08 Main Building, P. O. Box 938, Austin,Texas, 78712.

Effective Date of Contract:	September 12, 1968
Expiration Date of Contract:	August 31, 1971
Amount of Contract:	$55,943.04
Principal Investigators:	Lawrence Mann, Jr., and Myron H. Young
Telephone:	504-388-4428

TABLE OF CONTENTS

	Page
INTRODUCTION	1
Summary of Effort & Findings--Phase I	2
Summary of Effort & Findings--Phase II	3
TECHNICAL DISCUSSION OF WORK PERFORMED--PHASE III	15
REFERENCES	38
APPENDICES	39
DISTRIBUTION	71

LIST OF FIGURES

Figure	Title	Page
1	Original Experimental Configuration	4
2	Changes in Hardness vs Frequency - Run Two	8
3	Block Diagrams of Computer Analysis Configurations	11
4	Bar RA-Normal	12
5	Configuration Using Instron Testing Machine	16
6	Response of Bar Under Tension--Data of Runs Shown on Table 6	18
7	Plot of Data Shown on Table 7	21
8	Load vs Frequency for Various Bar Lengths	24
9	Frequency vs Length--Round Bars Before Correction	27
10	Frequency vs Length--Round Bars After Correction	28
11	No Load Round Bars Theoretical Study (D = .7078 in. L - Changes)	30
12	No Load Round Bars Theoretical Study (L = 12.037 in., D - Changes)	31
13	Horizontal Test Configuration for Thin Wall Tubing	36
14	Vertical Test Configuration for Thin Wall Tubing	37
15	Square Pulse - Input Spectrum	45
16	Square Pulse - Frequency Spectrum	46
17	Square Pulse - Power Spectrum	47
18	Sine Function - Input Spectrum	48
19	Sine Function - Power Spectrum	49

LIST OF TABLES

Table		Page
1	Frequency in Hertz with Orientations	6
2	Sample Hardness and Frequency - Run One	7
3	Sample Hardness and Frequency - Run Two	7
4	Differential Hardness vs Differential Frequency Run Two	9
5	Analysis of Variance	10
6	Least Squares Analysis for Data on Bar Shown in Table 7	17
7	Frequency vs Percent Yield	19
8	Experimental vs Theoretical Frequencies - Stress	20
9	Response Frequency for 1040 Bars Under Various Loads	23
10	Change in Length of Round Bar	26
11	Diameter Change of Round Bar	32

APPENDICES

Designation	Topic	Page
A	Analysis Theory and Data Reduction	39
B	Programming Theory	43
C	Stressed Bar Model Theory	52
D	1040 Stressed Bar Data	55
E	Theoretical Model to Develop Frequency on Non-Stressed, Simply Supported Bars	63
F	Computer Program	65

INTRODUCTION

In March of 1964 Louisiana State University initiated a Nondestructive Testing Institute. This institute was formed to foster interest in academic programs and in research in nondestructive testing. During the years of 1964 and 1965 the institute was mainly concerned with conducting short courses for civilian and service personnel in the field of nondestructive testing.

In 1966 application was made to the THEMIS program for a grant centering around nondestructive testing technology, One of the projects suggested was entitled, "Data Analysis and Correlation with Digital Computers". A portion of the project statement stated that: "Data correlation and analysis constitute one of the main links in the nondestructive experiment. Projects involving the response comparison of samples to a standard specimen in a vibrational type of test, or in a test by means of the reflection of ultrasonic waves, or in the back scattering test of nuclear radiation cannot reveal meaningful results unless proper interpretation of the signals from the sensors are made. These analyses can be efficiently handled by high speed digital computers using methods such as autocorrelation, Fourier transforms, and such statistical tests as the Chi Square".

The aims of that proposed project were compatable enough with the aims of the ARPA goals so as to be of interest to that agency. Thus the mutuality of interest resulted in the project described here.

The long range objective of the project was to develop a system whereby a digital computer can discern the difference between satisfactory and unsatisfactory basic components and machine parts.

The project was divided into three phases:

Phase I--Phase I provided for the creation of a computer program to analyze and display data when steel rods were subjected to various energy exciting media. The investigation apparatus was constructed and proven.

Eight (8) months, effective September 12, 1968.

Phase II--The computer analysis proved to be dependable in reproducibility of the results from the experimental energy envelopes. The computer program was firmed-up although improvements in the program continued to be made throughout the life of the contract.

The ability of the system to differentiate between heat-treated and nonheat-treated samples was investigated. The sensitivity of the computer-program to determine changes in dimensions, structural integrity, and degree of stress was initiated.

Twelve (12) months, effective June 30, 1969.

Phase III--Investigations centered primarily around the determinations of the sensitivity of the system to detect dimensional changes and degree of stress in materials. Structural integrity was investigated. The results

of hardness tests in Phase II were encouraging enough so that they were continued in Phase III. Conversion to simulated on-line real time analysis was completed through the use of an existing hybrid computer system.

Phase III extended contract for additional fourteen (14) months.

In addition to the work plan described above the researchers investigated the applicability of the system to nondestructively test relatively long (4 feet) sections of thin wall, small diameter stainless steel tubing.

Summary of Effect and Findings--Phase I

At the beginning of the first phase of the effort it was necessary to design and construct the apparatus and instrumentation to accumulate and store data.

Prior to building the apparatus it was necessary to choose the types of machine elements which would be vibrated. It was decided to use Starrett tool steel machined bars. The bars were all 18 inches long and the cross-sectional dimensions range from ¼ inch by ½ inch to ½ inch square. A vise was procured to hold the bars while they were being vibrated. In order to lessen the damping characteristics of the vise, styrofoam inserts were used between the vise and the bars.

The next problem to be encountered was that of "ringing" the bars at the same spot with the same magnitude from the driving device. It was decided to use a solenoid to drive a threaded pin so as to ring the specimens uniformly.

To record the signals a Computer of Average Transients, (CAT), Model 1000 manufactured by the Technical Measurements Corporation, was obtained. The CAT Model 1000 has a time corresponding multi channel digital memory whose principal function is to recover repetitive transient signals from random background noise.

It has a cathode ray tube display which gives a visual indication of the wave pattern at the end of the accumulated sweeps. Additional output of paper tape printer was also used.

The Technical Measurement Corporation Model 500 Decimal Printer is a combination of the Hewlett Packard H51-565A Printer and the TMC Control circuitry. Basically, the Model 500 printer prints out the BCD (binary coded decimal) coded information stored in the CAT unit. The printer records the complete contents of the CAT memory, when directed by the analyzer print control. This permanent record is printed on 3-inch standard paper tape at the rate of 5 lines per second, the total 400 channel memory taking approximately 1 minute and 20 seconds to print out.

In Figure 1, A indicates the DC power supply, B shows the bar, C shows the Technical Measurement Corporation CAT unit, D is the General Radio Corporation sound level meter, E is the voltage supply for the microphone when it is being used as a pickup, and F is the Technical Measurement Corporation Model 500 Digital Printer.

In summary, the work accomplished during Phase I includes the checking out of the adaptability of the Fast Fourier Transform as an adequate analysis tool for the problem under consideration. Various forms of frequency energy envelopes were investigated and the power spectral representation appears to offer the most promising signature for comparison purposes.

The computer program for data analysis was written around the Fast Fourier Transform and the program proved effective for data analysis.

In order to accomplish reproducibility, changes had to be made in the area of basic experimental set-up, driving medium, recording technique, and record length, and analysis approach in establishing a firm signature.

Summary of Effort and Findings--Phase II

At the time of the initiation of Phase II a primary concern was to what extent the pickup system and the analysis program could discern geometric differences in tests specimens. However, the dimensionsl experiment was not carried out immediately due to the interest in the hardening determination by heat treatment. Although the goals of the two experiments might be different the same NDT technique was applicable since the basic principle of the investigation was based on the frequency determination of a vibrating body. The body vibrates as a whole in one of its natural modes. Many physical characteristics of the body may be determined from the characteristics of the induced vibrations. In most practical applications, the natural frequencies lie largely within the audible range, from a few to about 20,000 cycles per second.

When a thin bar is subjected to a light tapping impulse, produced by an electronically controlled plunger, it response is equivalent to the response of a first order system and is identical with its natural motion from an initial position. A first-order system is one whose motion can be expressed by a first-order constant coefficient differential equation. Since the impulse generates a very short-time initial condition, the response produced is the natural vibration of the bar. The resulting natural frequency is sometimes referred to as the resonant frequency, which is the frequency when the body is subjected to a forced vibration whith the same frequency as its natural frequency.

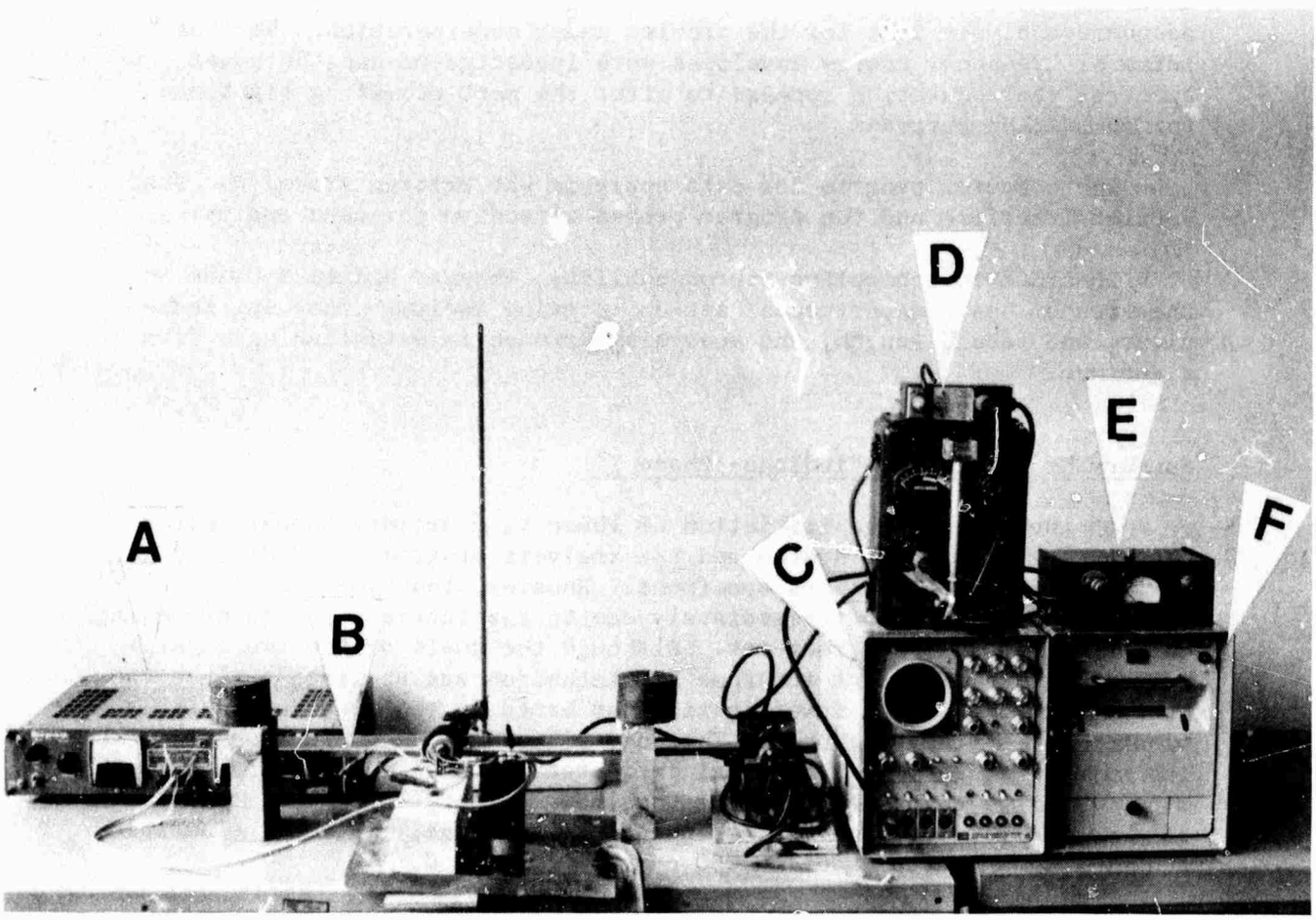

Figure 1

Original Experimental Configuration

The natural frequency of mechanical vibration of a homogeneous body is controlled by a number of factors which may be generalized by 2 factors in the expression:

Frequency = (shape factor) x (physical-constants factor)

Shape factor includes the geometric design of the body and the dimensional factors of length and thickness. The physical-constants factor includes the modulus of elasticity, density and Poisson's ratio for the test material.

It is axiomatic that two bodies, identical in every respect, will manifest identical natural frequency in vibration. If the shape factor of a number of bodies is held constant, the natural frequency of vibration of each of the bodies will be a discrete measure of the physical-constants factor. On the other hand, if the effect of the shape factor on frequency can be determined, compensation for differencies in shape or size may be applied.

Every object has many modes of vibration. In addition to the fundamental mode it maybe expected that the complexity of modes and overtones would complicate the resonance vibration test. However, it is not the case in this experiment because the impulse excitation would not excite the higher order overtones at a simply supported configuration. The fundamental frequency of vibration is usually the most conveniently detectable frequency.

Vibration testing was used in flaw detection by others. McMasters[1] reported the example of the flaw simulated by a lateral saw cut in the center of a square bar. The method of detecting the flaw consisted of measuring the response frequencies of the fundamental mode after placing the bar into separate orientations. Table 1 was prepared from actual measurements of a simulated and progressively deepened flaw.

It can be seen that there is a difference in the response frequency as the depth of the flaw increases.

The hardening of a steel specimen by heat treatment could be thought of as a body experiencing uniform microscopic flaws. When steel is in the non-hardened conditions it is essentially pearlite. This microstructure is a laminar mixture of ferrite and carbide. The lighter color is the ferrite and the darker color is carbide. There is nearly 12% carbide and slightly more than 88% ferrite in the mixture. Since the carbide and ferrite form simultaneously, they are intimately mixed. Characteristically the mixture is laminar. That is, it is composed of alternate layers of ferrite and carbide. The resulting microstructure is called austenite.

---

[1] McMaster, Robert C., Nondestructive Testing Handbook, Vol. 2, page 51-12.

TABLE 1

Frequency in Hertz with Orientations*

Depth of Flaw, in.	A	B	Frequency Difference
0	1552	1552	0
1/16	1533	1541	8
1/8	1469	1533	64
3/16	1400	1513	113
1/4	1327	1507	180

*Orientations of the same bar are different. Position A is horizontal. Position B is vertical.

After heat treatment, as temperature decreases the free energy difference between the austenite and the combination of ferrite plus carbide becomes larger. Consequently, the austenite is more unstable. At sufficiently low temperatures, but usually still above room temperatures, the face-centered structure does change to a body-centered structure, but all of the carbon present remains in solution. Consequently, the resulting body-centered structure is tetragonal rather than cubic. It is then called martensite.

Since martensite has a noncubic structure it is reasonable to expect that any energy signature obtained from a cubic structure then noncubic structure would have a differential. It is believed that this difference in structure results in the difference in frequency. Until further work is done it can not be argued that the frequency is entirely attributable to grain structure. It might be attributable to the resulting stresses set up in the steel.

The first three months of the Phase II were spent in continuing development of the system procedure to differentiate between very small changes in configuration and integrity of the steel bars that were being tested. During that time period the ability to reproduce results, when the same bar is vibrated after being removed from the holder and reinserted in the holder, was perfected.

Following that, investigation into the ability of the system to determine a frequency correlation of a sample after being heat treated was initiated. The first step consisted of choosing two bars and subjecting them to the computer analysis both before and after heat treating. The results offered enough promise to pursue the problem. The second step consisted of fabricating eight sample bars, each eighteen inches long from the same piece of one-half inch bar stock.

The bars were subjected to a Brinell hardness test to determine their before heat treated hardness. Energy signatures were then made of each bar and the bars were then heat treated. After heat treating, the hardness of the bars was again determined and the energy signatures again recorded. The bars were then X-rayed to determine if there were any discontinuities introduced as a result of the heat treating operation. Table 2 shows the results of these determinations.

TABLE 2

Sample Hardness and Frequency--Run One

Rod Ident.	Brinell before H.T.	Brinell after H.T.	Response freq. before H.T., Hertz	Response freq. after H.T.,Hertz
F	57.7	56.2	588	584
G	61.0	59.0	588	580
H	58.4	60.3	592	588
I	59.7	61.0	592	580
J	57.8	54.5	592	576
L	58.4	58.8	588	580
M	59.2	55.1	592	572
N	59.7	58.0	592	584

It will be realized that the magnitude of the hardness differences encountered in the sample were slight. The trend of the tests suggested that some correlation between hardness and frequency response of the samples. Little credence was given to these results since certain errors became apparent after the runs were made.

Therefore, in order to verify the relationship, another set of samples was prepared. This time the samples were made from 1095 stock, a steel more conducive to heat treating than the 1020 used in run one. These are prefixed by the letter "A". Figure 2 describes the data collected during this experiment.

TABLE 3

Sample Hardness and Frequency--Run Two

Rod Ident.	Response freq. before H.T.,Hertz	Response freq. after H.T., Hertz	Rockwell C, before H.T.	Rockwell C, after H.T.
AA	945.3	937.5	8.6	42.6
AB	960.9	947.3	8.6	36.5
AC	957.0	945.3	8.6	36.5
AE	953.1	945.3	8.6	27.3
AG	960.9	945.3	8.6	47.5
AH	946.3	921.9	8.6	54.0
AI	968.8	953.1	8.6	33.1
AJ	945.3	937.5	8.6	36.9
AK	945.3	937.5	8.6	6.0
AL	937.5	937.5	8.6	2.2

FIGURE 2

CHANGES IN HARDNESS VS FREQUENCY-RUN TWO

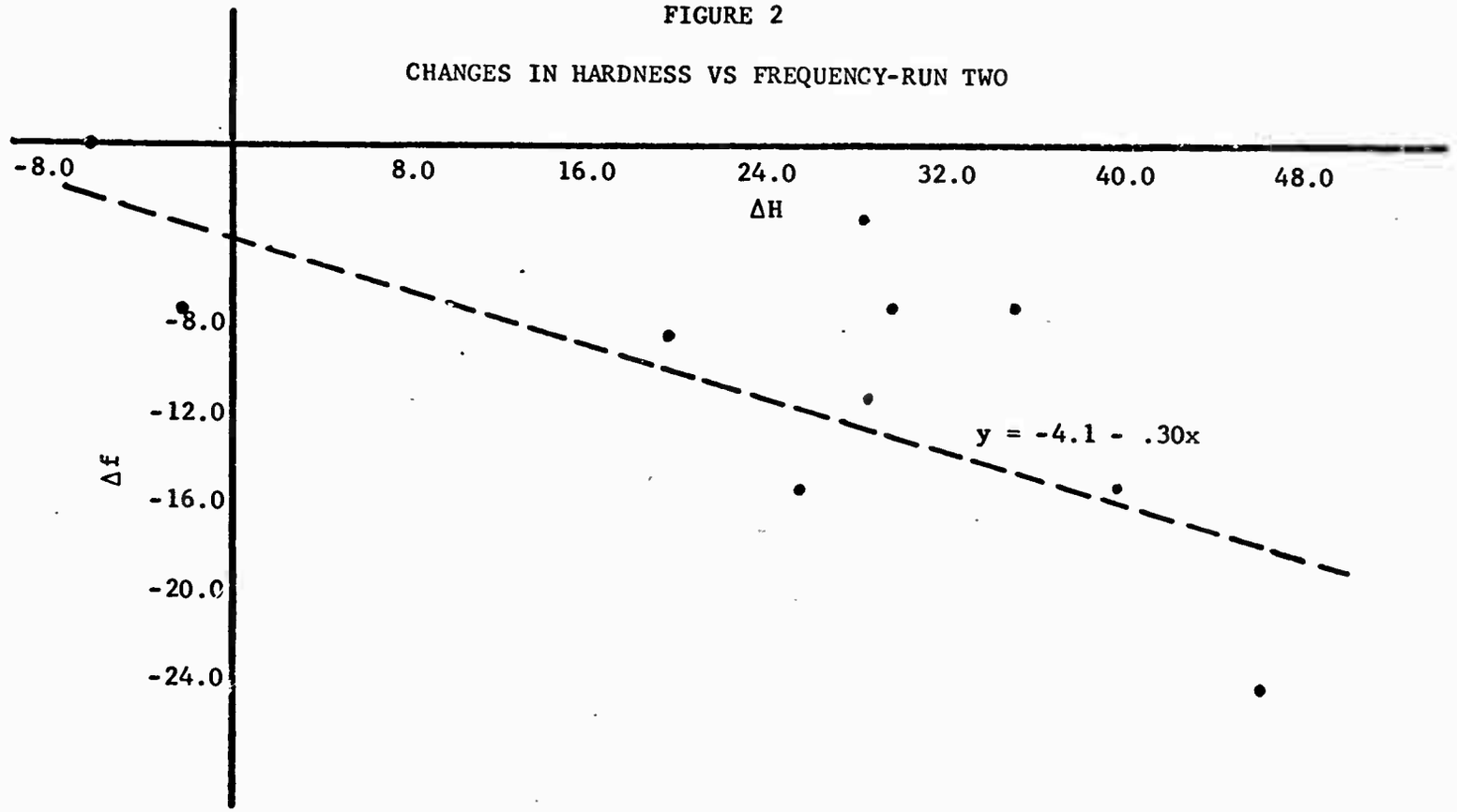

Table 4 reduces the data in Table 3 to a differential hardness related to a differential frequency and this information is plotted on Figure 2.

Figure 2 indicates the data collected. The degree of relationship between the two above mentioned variables is shown below.

The data shown in Figure 2 was obtained by taking 10 bars and subjecting these bars to various degrees and intensities of heat treatment.

TABLE 4

Differential Hardness vs. Differential Frequency--Run Two

Rod	Δ Hardness, Rockwell C, after-before	Δ Frequency, Hertz after-before
AA	34.0	-7.8
AB	27.9	-3.6
AC	27.9	-11.7
AE	18.7	-8.8
AG	38.9	-15.6
AH	45.4	-24.4
AI	24.5	-15.7
AJ	28.3	-7.8
AK	-2.6	-7.8
AL	-6.4	-0.0

The data were subjected to a conventional correlation-regression treatment to obtain a mathematical model. The model is:

$$y_i = -4.11 - .30x$$

with a coefficient of correlation of .78, where the variables are as defined previously.

The analysis of variance of regression is as follows:

TABLE 5

Analysis of Variance

Source	Degrees of Freedom	Sum of Squares	Mean Square	F Ratio
Regression	1	232.3	232.3	12.1
Residual	8	153.3	19.2	
Total	9	385.6		

During Phase II it became apparent that, for the data analysis system to be of any practical use, a faster system should be sought. Coincidental with this realization, the LSU hybrid computer system became operational. This computer, supported by the Department of Defense, under a THEMIS grant, involved an expenditure of over $750,000 for hardware alone.

A hybrid system receives analog information such as voltages which are, in this case, proportional to the sound signature. The LSU hybrid system uses a Sigma 5 for the digital component and an EAI 680 for the analog component. Using the hybrid system, it is necessary merely to record on magnetic tape, one cycle of an energy signature. The tape is then used as input to the hybrid system. Figure 3b depicts, in block diagram form, the schematic of the hybrid analysis. The digitizing interval can be varied by a simple change of circuit elements. The play back speed can also be varied. The analog signal is converted to digital information through an A to D converter (ADC). This information is in turn stored sequentially in the memory core of the digital part of the hybrid computer. As soon as a preset number of sampling points are obtained, the calculations begin. The final result can be either display on an oscilloscope, or on a x-y plotter, or on a print plot. The print plot was chosen because of its simplicity and clarity of locating the resonance peak. It is also the fastest way to obtain a permanent record.

In an attempt to verify the computer program for the hybrid system, the signature of a pulser generated frequency (625 Hertz) was run on the hybrid system. A portion of the results are shown on Figure 4. It has been shortened for presentation purposes and the line connecting the "P's" has been drawn in for clarification. This printout is analogous to that obtained from the calcomp x-y plotter used with the previous system.

In Figure 4 the N is the number of digitized sampling points of the sound signature. LG (LAG) is the autocorrelation lag. TIME RES. is the time interval between sampling points in milliseconds. The Nyquist frequency is the maximum frequency that can be observed with the given time resolution. FREQ. RES. is the frequency resolution interval between consecutive points in the power spectrum. The R column is the list of normalized autocorrelation function values. The P column is the list of normalized power spectral values.

FIGURE 3

BLOCK DIAGRAMS OF COMPUTER ANALYSIS CONFIGURATION

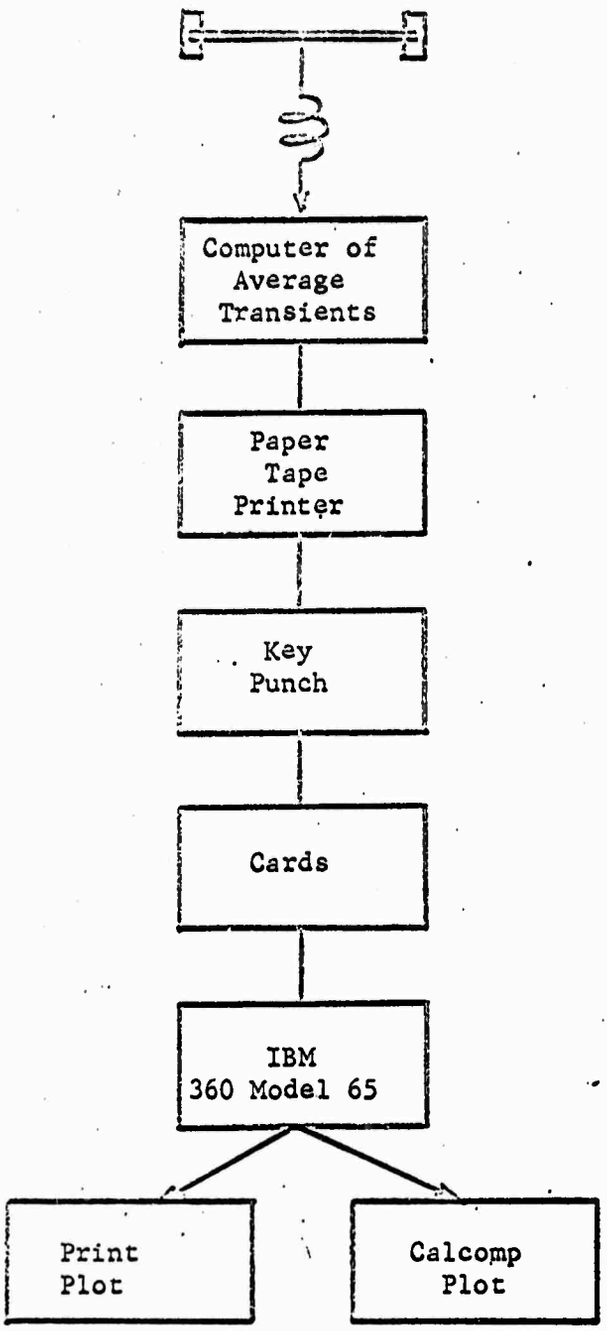

(a)

Original Method

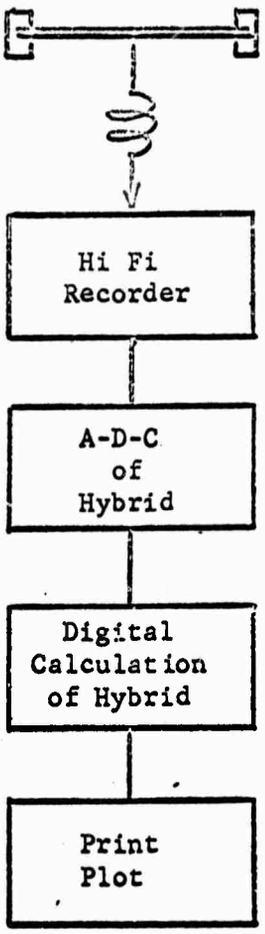

(b)

Hybrid Configuration

FIGURE 4

BAR RA-NORMAL

N = 3000 LG(LAG) = 256 TIME RES. = .4000 MSEC NYQUIST FREQ. = 1250 HZ FREQ. RES. = 9.7656 HZ R SCALE = 150002.2500 P SCALE = .2414

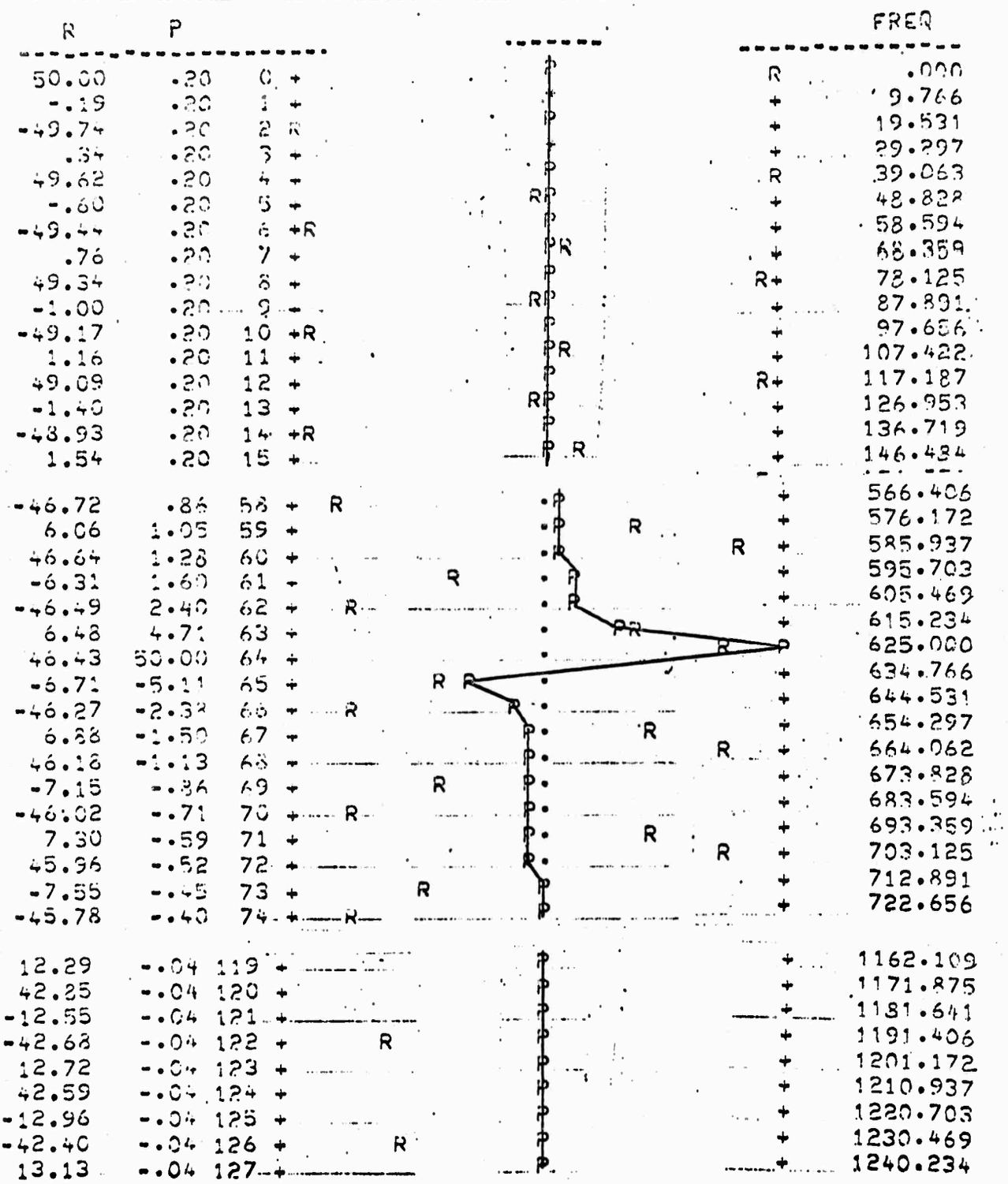

The ratio of P/(P SCALE) (see heading for P SCALE) gives the actual P value calculated. The ratio of R/(R SCALE) (see heading for R SCALE) gives the actual R value calculated. The * indicates P and R coincide. The autocorrelation function is used to indicate the degree of constancy of a particular signal quantity as a function of time. The power-density spectrum, which represents a measure of the distribution of energy in the frequency spectrum, is the Fourier transform of the autocorrelation function.

The programming and theoretical considerations resulting from Phase II are included in Appendix B.

A number of conclusions were drawn from the work performed during Phase II.

1. There appeared to be a predictable relationship between changes in the hardness of certain carbon steels and changes in response frequencies.

2. Hybrid computational equipment can give on-line analyses of these situations.

3. Frequency changes could be attributable to differences in hardness and stress differences.

In any experimental investigation such as that described here, a mathematical model is sought to define the cause and effect aspects. Ideally, if a coefficient of correlation of 1.0 would be obtained, it could be assumed that only a change in hardness causes a change in response frequency. In run two, a coefficient of correlation of .78 indicates that, to some small degree, other factors are present. One of these factors might have been the sample size. The other might have been the fact that a variable or variables other than hardness is causing a change in frequency. But, in view of the coefficient of correlation obtained, the majority of the variation is probably accounted for by a change in hardness alone.

The procedure used for analysis during Phase II consisted of collecting the energy signatures, averaging a number of them, and then digitizing them on paper tape. Cards were then cut from the paper printout tape and the data run on the program using the IBM 360 Model 65 system. This was a time consuming process requiring averaging 3 days from data acquisition to receipt of plots. With the program prepared during Phase II, every indication pointed to the successful adaption to the existing LSU hybrid computer to analyze the data. It was still, however, a simulated on-line system since a sound recording tape was used to record the sound and it had to be transferred to the hybrid system to be analyzed. If tape could be eliminated, the direct sound signature results could be obtained immediately. This would change from a simulated on-line system to a truly on-line system, that is, results could be obtained within one minute or less after vibration of the sample.

Following the frequency-hardness investigations, the frequency-dimension project was started during Phase II.

Fourteen bars were cut and end center drilled for a lathe mounting. The diameter of each bar was reduced incrementally to ascertain the sensitivity of the analysis procedure to react to dimensional differences. These runs were made on the hybrid system.

Fourteen rectangular bars were prepared to stress using a tensile testing machine. Before and after signatures were made to determine whether or not the procedure, as developed, could differentiate between the before and after case and the nature of that relationship. Results of this work are described in the next section.

TECHNICAL DISCUSSION OF WORK PERFORMED

PHASE III

During Phase III, the following topics were investigated.

1. The stress analysis was completed on twenty rectangular bars (six 1010 carbon steel and fourteen 1040 carbon steel). The results indicate that there is a promising relationship between the stress and resulting frequency of the bars and that this relationship is only negligibly dependent on the dimensional changes of cross-sectional area and the bar length that result from the stress.

2. A non-stress analysis of the dimensional property of length was performed on a carbon steel round bar to ascertain the effect of a change in length while the diameter remained unchanged. During this period a frequency resolution improvement was made to the computer program to give more sensitive results. This fact added to the attractiveness of the acoustic technique.

3. An analysis of the dimensional properties of the diameter of a non-stress carbon steel round bar was performed to ascertain the effect of a change in diameter while the length remained unchanged.

4. Rolled steel specimens were tested to ascertain if the hardness could be determined by the acoustical technique. These specimens were received from Frankford Arsenal.

5. An attempt to use the acoustical technique to monitor the integrity of long, thin wall, small diameter tubing was made. The stainless steel tubes were sent from WADCO (a subsidiary of Westinghouse Electric Corporation) in Richland, Washington.

6. A 1/60" hole was drilled through the diameter center axis of two round, carbon steel bars to determine if a frequency change would result between them and integral bars.

Stress Analysis

The stress analysis investigation was initiated by loading a 1010 carbon steel rectangular bar on the Instrom tester model TT type D. Figurge 5 shows this experimental configuration. The bar was loaded by applying increasing tensile stresses in percentages of its yielding stress. At each increment the bar was struck by the solenoid and the resulting sound was recorded on the tape recorder. This recording was then introduced into the hybrid computer to be analyzed. The response frequency of the bar was determined and printed. Six 1010 carbon steel, rectangular bars were tested in two groups of three. The results of group one are listed in Table 6 with the resulting curve in Figure 6. Once the configuration for group one was established, group two was then run with more attention paid to detail.

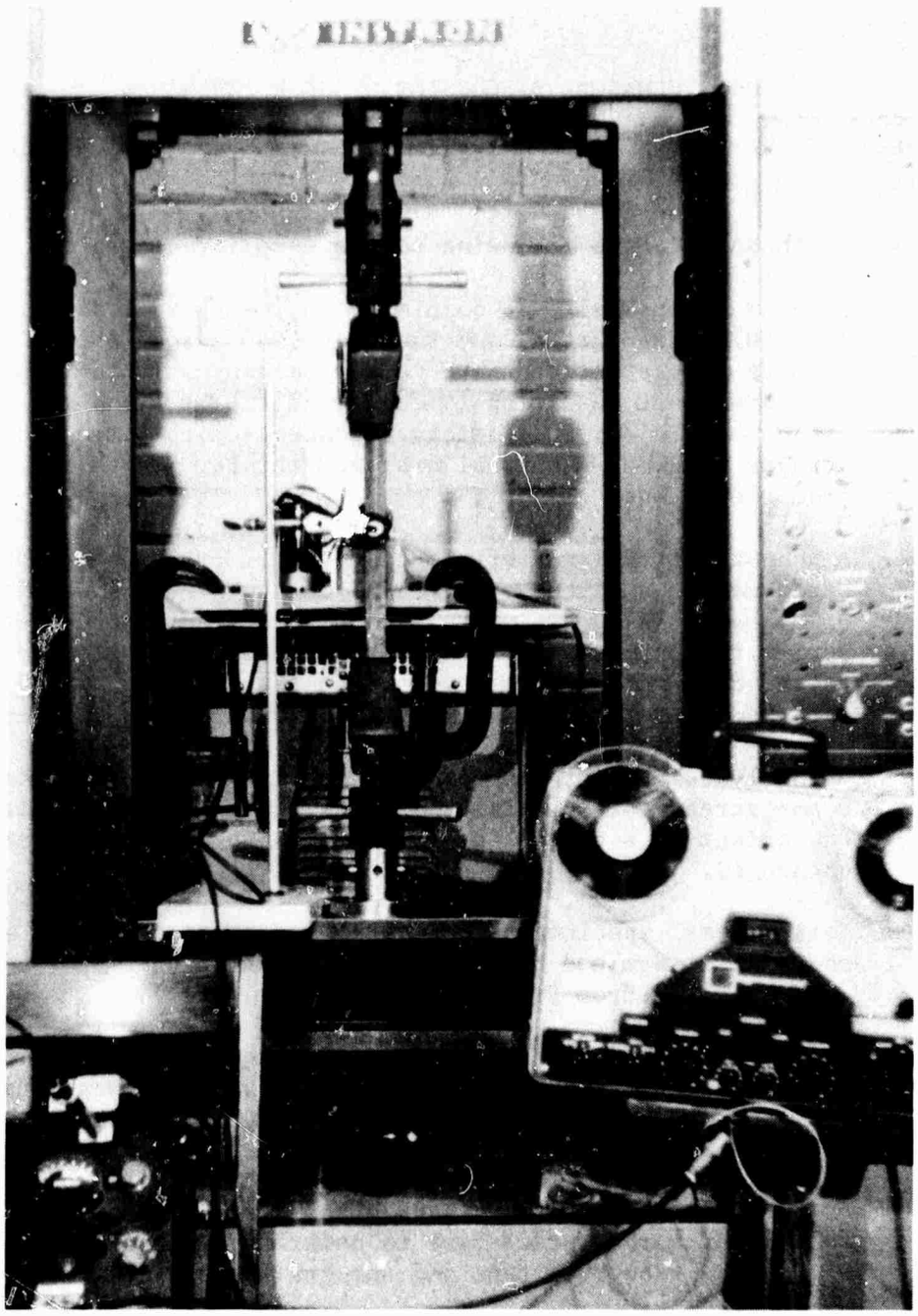

Figure 5

Configuration Using Instron Testing Machine

This data is shown in Table 8. A curve of the results is shown in Figure 7. Note the relation between the experimental and theoretical frequencies. The theoretical model is developed in Appendix C.

TABLE 6

LEAST SQUARES ANALYSIS FOR DATA ON BARS

SHOWN IN TABLE 8

y = % Yield

	x = Exper. Freq.	x = Theoretical Freq.
Bar I	y = 143.5 + .588 x R = .99	y = 126.18 + 1.59 x R = .99
Bar II	y = 133.6 + .63 x R = .99	y = 124.3 + 1.72 x R = .996
Bar III	y = 138.2 + .49 x R = .98	y = 122.6 + 1.75 x R = .99

Figure 6

RESPONSE OF BAR UNDER TENSION

DATA OF RUNS SHOWN ON TABLE 8

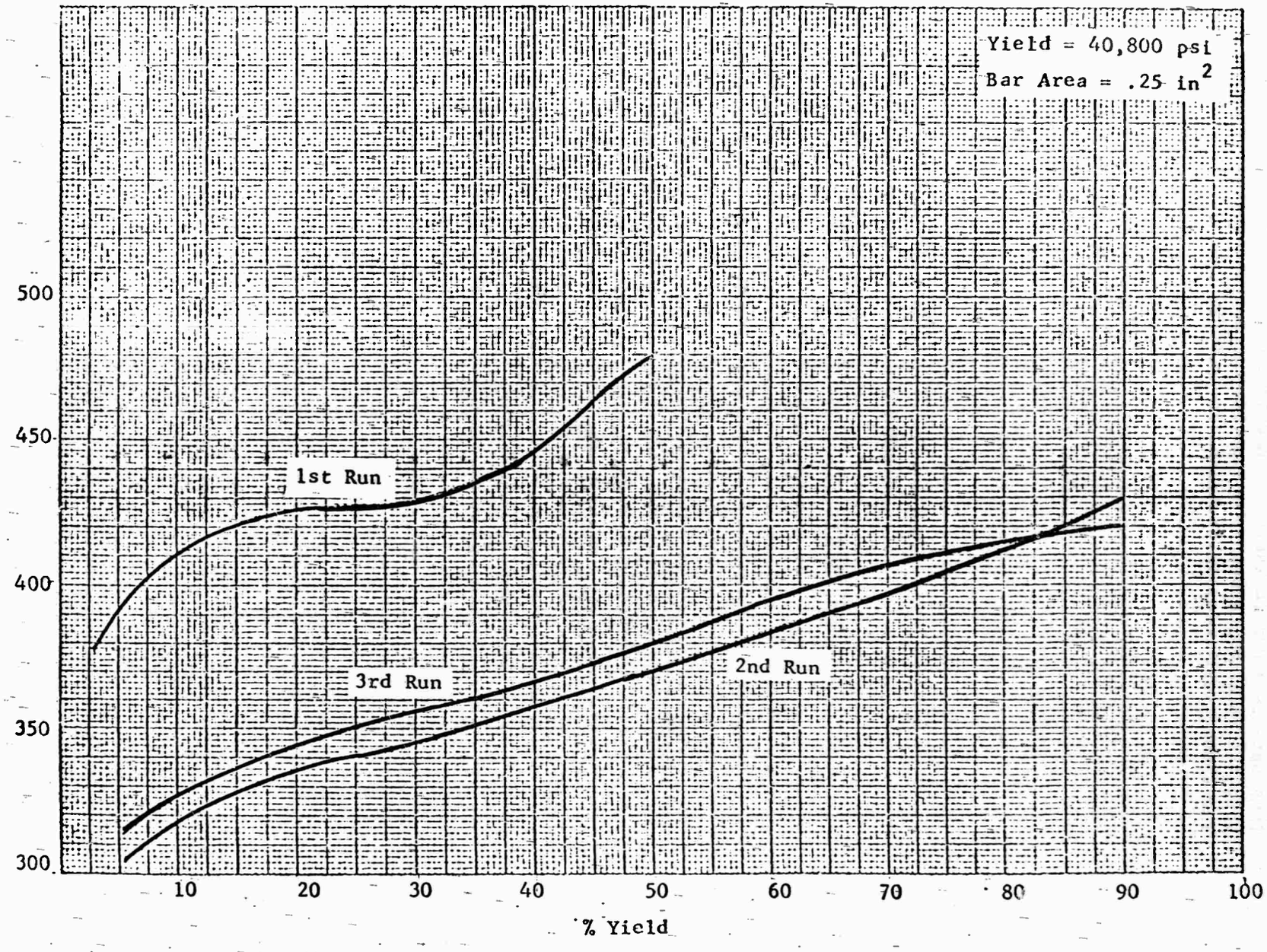

TABLE 7

FREQUENCY VS PERCENT YIELD

% Yield	Freq. 1st Run Approx. 12" Clear Between Grips	Difference in Frequency	Freq. 2nd Run Approx. 13" Clear Between Grips	Difference in Frequency	Freq. 3rd Run Approx. 13" Clear Between Grips	Difference in Frequency
5	390	20	304	16	312	16
10	410	18	320	15	328	15
20	428	0	335	8	343	16
30	428	20	343	16	359	8
40	448	20	359	16	367	15
50	468		375	7	382	16
60			382	16	398	8
70			398	16	406	8
80			414	7	414	15
90			421		429	

Squares Analysis:

y = 389.14 + 1.53 x	y = 304.1 + 1.34 x	y = 314.5 + 1.30 x
R = .972	R = .996	R = .99

y = % yield

x = exper. freq.

R = correlation coeff.

TABLE 8

EXPERIMENTAL VS THEORETICAL FREQUENCIES-STRESS

Bar I
460 g

% Yield	Load	Width	Depth	Length	Exper. Freq.	Theoretical Freq.	
0		.9897	.2518	11.324		117	y = 126.18 + 1.59 x
5	500	.9887	.2518	11.326		131	R = .99
11	1020	.9885	.2515	11.326	148	144	
23	2050	.9887	.2518	11.330	156	167	
34	3050	.9890	.2515	11.334	164	186	
44	4000	.9885	.2516	11.335	171	203	
57	5100	.9887	.2517	11.337	179	221	
68	6100	.9890	.2515	11.340	187	235	
80	7130	.9888	.2514	11.346	187	250	
90	8040	.9895	.2515	11.350	195	262	

Bar II
447 g

0	25	1.002	.2521	11.682	132	119	y = 124.3 + 1.72x
10	900	1.002	.2521	11.687	140	142	R = .996
20	1820	1.0018	.2520	11.690	148	162	
30	2700	1.0020	.2520	11.693	156	181	
40	3600	1.0015	.2519	11.698	156	197	
50	4500	1.0018	.2519	11.700	164	212	
60	5400	1.0015	.2519	11.700	171	227	
70	6300	1.0015	.2519	11.702	179	240	

Bar III
455 g

0	100	.9982	.2521	11.796		119	y = 122.6 + 1.75 x
10	900	.9980	.2520	11.800	140	140	R = .99
20	1800	.9980	.2520	11.808	148	160	
30	2700	.9975	.2520	11.812	156	178	
40	3600	.9970	.2520	11.814	156	195	
50	4500	.9965	.2519	11.815	164	210	
60	5400	.9965	.2519	11.818	171	224	
70	6300	.9965	.2519	11.822	171	238	
80	7200	.9962	.2519	11.829	179	251	
90	8100	.9962	.2519	11.836	179	263	

y = 143.5 + .588 x, R = .99

y = 133.6 + .63 x

y = 138.2 + .49 x, R = .98

y = % yield; x = exper. freq.; x = theoret. freq.

FIGURE 7

Plot of Data Shown on Table 8

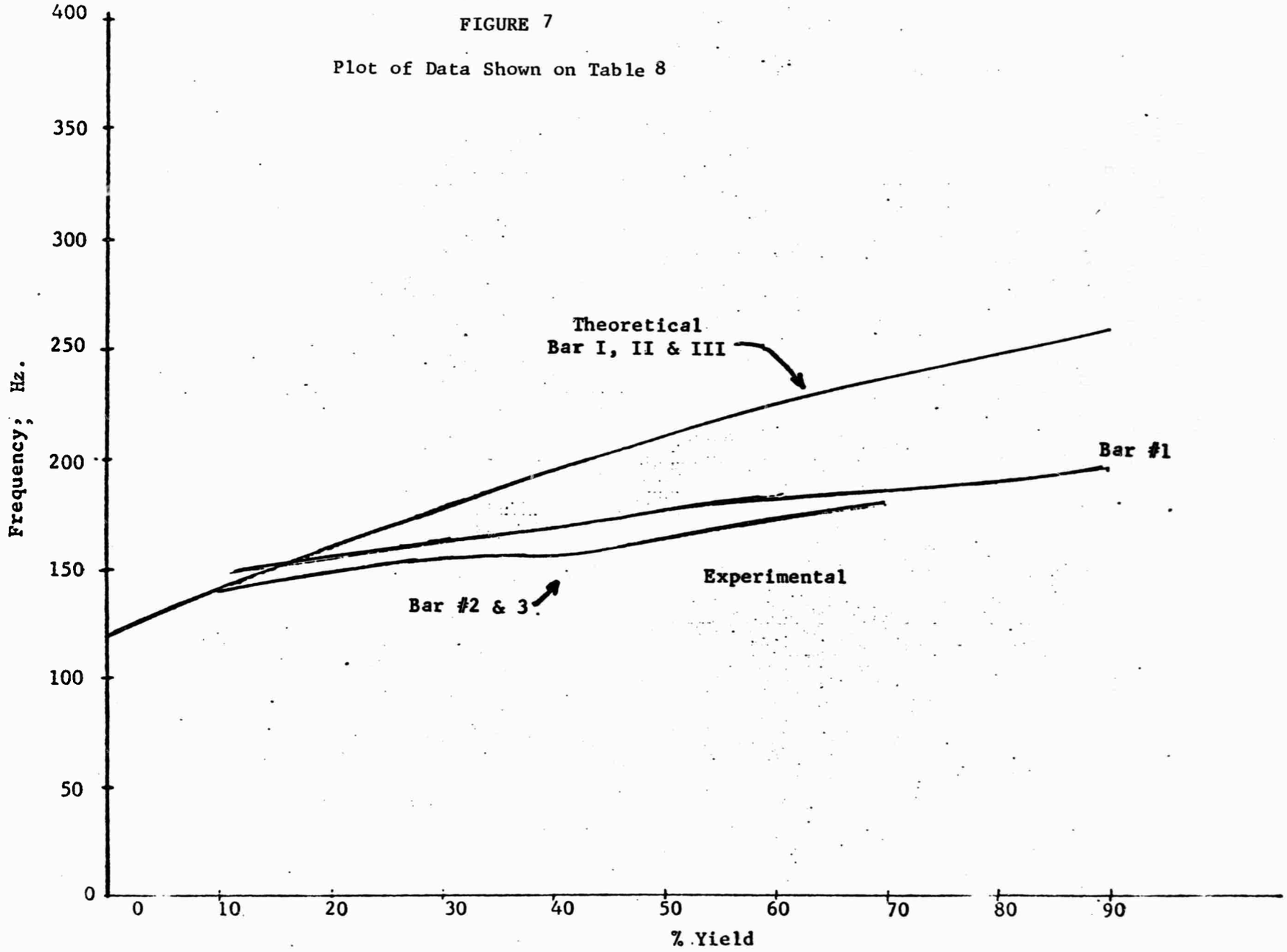

Fourteen 1040 stainless, carbon, rectangular steel bars were then run to determine whether the frequency change was due to a change in cross-sectional area or change in stress. The bars were tested in the same manner as the 1010 carbon steel bars referenced to previously. However, because they were essentially strainless, their cross-sectional area had little (.3%) measurable change. Due to this property of the bars, the results indicate that the relationship is mainly between stress and response frequency of the bars. The data and results for these bars are listed in Table 9 with an accompanying curve in Figure 8. The complete data on this run is included in Appendix D.

TABLE 9

RESPONSE FREQUENCY FOR 1040 BARS UNDER VARIOUS LOADS

BAR NUMBER

	1	2	3	4	5	6	7	8	9	10	11	12	13
1,000	257	355	343	351	343	335	328	328	296	347	281	339	339
2,000	367	355	292	375	371	289	277	363	367	367	367	367	367
3,000	382	371	257	390	386	375	375	378	382	382	382	382	382
4,000	398	382	234	402	398	386	390	390	394	398	398	394	394
5,000	410	394	203	417	417	203	406	406	406	410	410	410	410
6,000	425	414	414	429	425	414	417	417	421	421	425	421	421
7,000	1914	988	425	1914	441	425	433	433	437	437	437	437	437
8,000	--	964	957	1944	1928	441	441	445	449	937	929	933	449
9,000	1968	945	933	1976	1960	453	1914	1898	1914	910	910	917	910
10,000	1984	929	917	1992	1984	917	1928	--	898	898	890	1078	894

Figure 8

Load vs. Frequency For
Various Bar Lengths

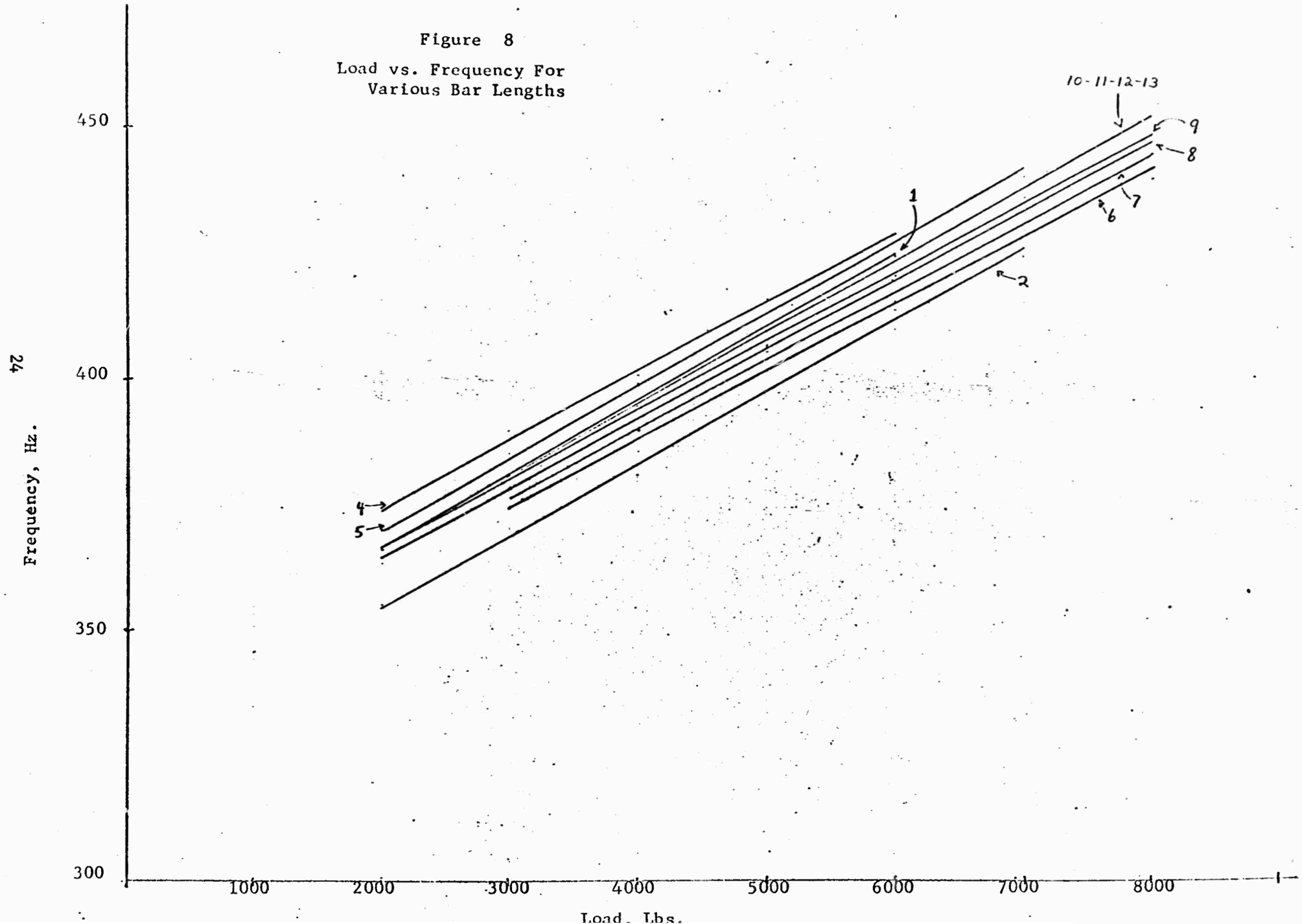

Dimensional Study

A. Length Variation

In search for the correlation between the length of a bar and its response frequency, a round carbon steel bar, approximately 12" long was prepared. It diameter was constant. The bar was freely supported at two ends with ¼" styrofoam in contact at each end. There was no rigid restrain at the supporting ends. The weight of the bar and the friction at the ends are the only means to keeping the bar in position when struck from the side at its midpoint by the solenoid plunger. The energy envelope of the bar was recorded and analyzed. The frequency of the bar at each decremental length was obtained and the results tabulated in Table 10. The relationship between the experimental frequency and the length appear in good agreement with the theoretical model. The theoretical response frequency of a round bar with hinged ends is (see Appendix E).

$$f = \frac{n^2\pi}{2L^2}\sqrt{\frac{EI}{\rho}} \qquad (1)$$

in which, $I = \pi D^4/64$ for round bars. The length and frequency relationship becomes

$$f = \frac{\pi D^2}{16(L/n)^2}\sqrt{\frac{\pi E}{\rho}} \qquad (2)$$

If all terms are held constant except the length and the frequency, their relationship is

$$f \sim \frac{1}{L^2}$$

The experiment result verified this inverse square relationship. However, the magnitude of the experimental and theoretical frequencies disagreed by a constant factor. Both theoretical and experimental frequencies plotted as a function of length are shown on Figure 10. Further study of this discrepancy reveals that the factor n in Equation (2) played an important role in the analysis. n indicates whether the bar vibrates in a fundamental mode with $n = 1$, or in the second harmonic with $n = 2$, or in higher order harmonics with $n > 2$. When $n = 1$, the vibration has nodes at 0 and L. This is a hinged-end model. When $n = 2$, the nodes are at 0, L/2 and L. The experimental result indicated that the n value was between 1 and 2. The reason for the perculiar node positions resulted from the bar supports. They were

not hinged ends. The bar ends were free to vibrate on the surface of the styrofoam when the bar was struck at midpoint from the side. The distance between the nodes was found to be 0.662 L. This means n = 1.5186. With this new value of n, the theoretical curve coincided with the experimental curve. These are illustrated in Figures 9 and 10. For this reason, if the experimental set up was a hinged end configuration, the experimental frequencies would agree with the n = 1 theoretical values.

TABLE 10

CHANGE IN LENGTH OF ROUND BAR

DIAMETER 0.7000"

X Length In	Weight Grams	y_2 Theoretical	y_1 Frequency, Hz Experimental
12.043	595	384	883
11.945	590	390	898
11.844	585	397	932
11.736	580	404	942
11.626	575	412	951
11.535	570	418	966
11.438	565	425	981
11.315	560	434	996
11.186	555	444	1020
11.064	545	455	1035

Least Squares Analysis with a linear model:

Experimental $y_1 = 2700.3 - 150.34\ x$

$R = -.99$

Theoretical $y_2 = 1245.2 - 71.62\ x$

$R = -.997$

During this period of the experiment the computer program sensitivity has been improved. It is known that the frequency resolution limitation had an effect on the sensitivity of obtaining the experimental frequencies. The experimental frequency calculations are based on the power spectural analysis

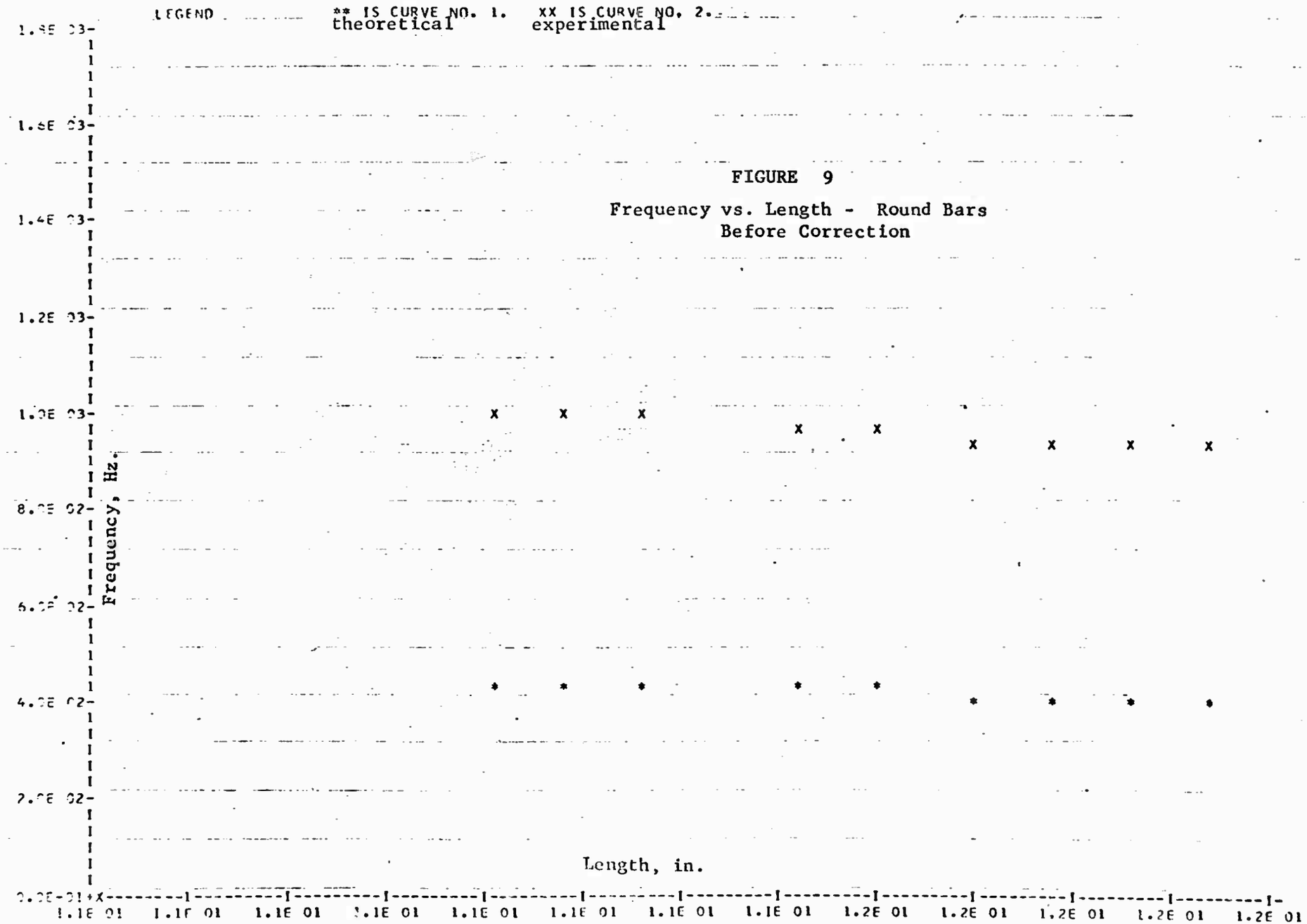

FIGURE 9

Frequency vs. Length - Round Bars
Before Correction

FIGURE 1, STEEL BAR STUDY FOR ROUND BARS. (D = CONST., L - CHANGES)

HORIZONTAL SCALE 0.70E-01 PER INCH
VERTICAL SCALE 0.20E 03 PER INCH

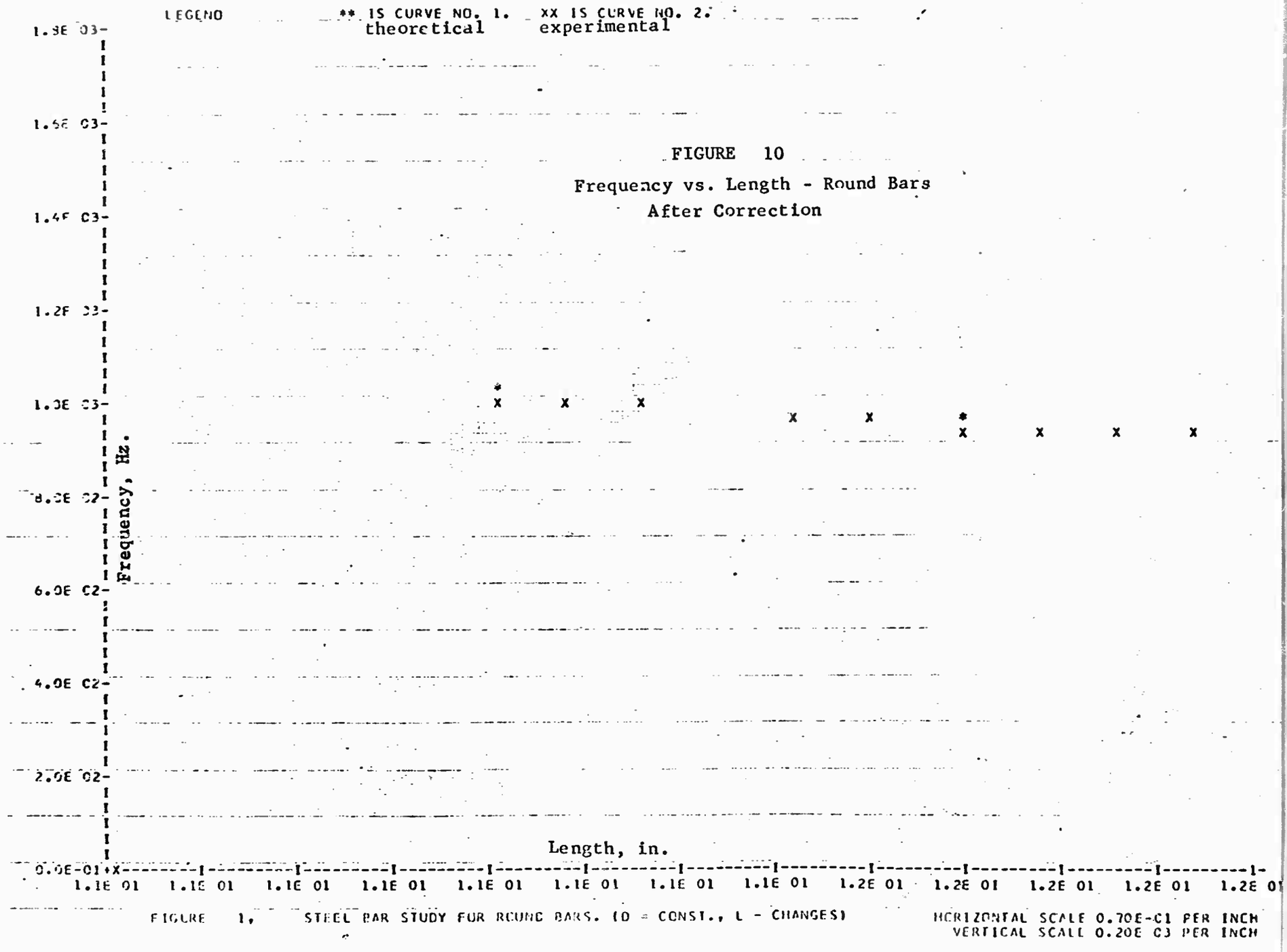

FIGURE 10

Frequency vs. Length - Round Bars
After Correction

FIGURE 1, STEEL BAR STUDY FOR ROUND BARS. (D = CONST., L - CHANGES)

HORIZONTAL SCALE 0.70E-01 PER INCH
VERTICAL SCALE 0.20E 03 PER INCH

of the time-series data. The final frequency resolution, which is the smallest frequency change that can be resolved, is a function of sampling interval of the analog data and the maximum lag of the autocorrelation function. If the sampling interval is made large, the Nyquist frequency will be lowered. However, the frequency resolution will be improved. If the response frequency of the bar continue to fall within the lowered Nyquist frequency, it appears wise to increase the sampling interval for the analog-to-digital conversion. The other approach was to increase the maximum lag number of the autocorrelation function. However, since the Hybrid computer has a limited storage location (32 K memory), an increase of the maximum lag from 256 to 512 will over fill the core storage. Since a 256 to 512 increase is a minimum step increase, the alternative remedy is to reduce the sampling record. Three thousand points of information were gathered for each run. Since the nature of the data is a transient one, 1000 to 2000 points may suffice. A modification of the computer program has achieved this goal and is reproduced as Appendix F. It was found that by increasing the sampling intervals from 0.4 msec to 0.5 msec, a reduction of frequency resolution from 8.9 Hz to 7.8 Hz was produced. Further reduction was made by revising the computer program to give a greater max lag in correlation analysis. The result gave a 3.9 Hz resolution. However, the Nyquist frequency was limited to 1000 Hz. The summary of the sampling time, max lag and frequency resolution is shown as follows:

Sampling Time (msec)	Maximum Lag	Frequency Resolution (Hz)	Nyquist Frequency (Hz)
.4	256	9.7656	1250
.4	512	4.8828	1250
.5	256	7.8125	1000
.5	512	3.90625	1000

B. Diameter Variation

Similar efforts have been made for the correlation between the diameter of a bar and its response frequency. A carbon steel round bar was prepared for the experiment by altering its diameter on a lathe while the length remained constant. The diameter was cut in decrements from 0.7078" to 0.6150". The results are tabulated in Table 11. In view of Equation (2), the response frequency should be directly proportional to the square of the diameter if all other terms are held constant.

In order to make a comparison of both varying length and varying diameter, theoretical curves are plotted with extended dimensional decrements. These are shown as Figures 11 and 12. On Figure 12 a linear regression analysis was made to both experimental and theoretical curves. The slope of the experimental curve is 1169.6 and the slope of the theoretical curve is 1268.7. This agreement appears most satisfactory for the sample size used. Note that the theoretical curve was obtained with n = 1.5186 same as the length varying case.

Figure 11.

No Load Round Bars Theoretical Study
(D= 0.7078 in. L- changes)

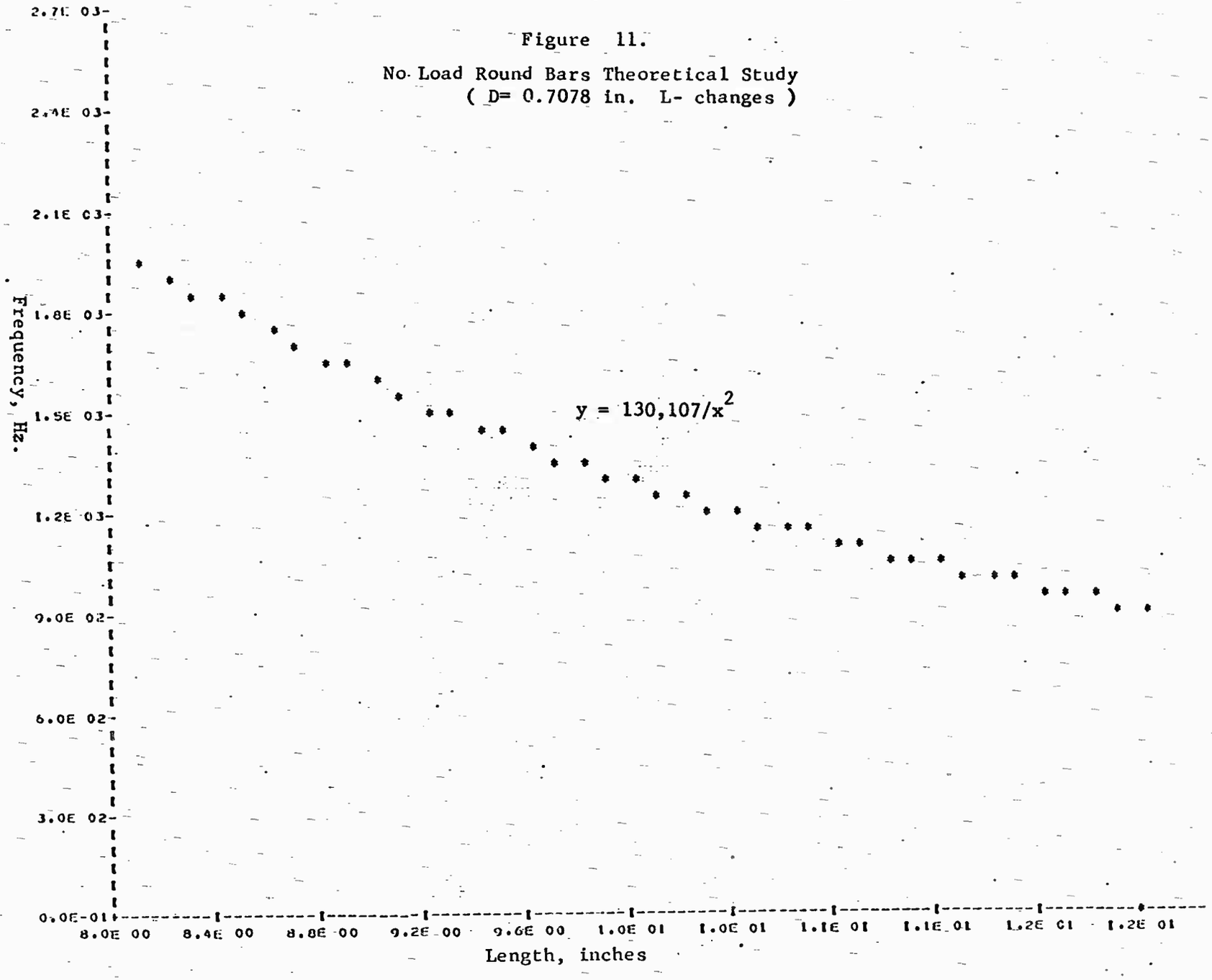

Figure 12.

No Load Round Bars Theoretical Study

(L = 12.037 in., D - changes)

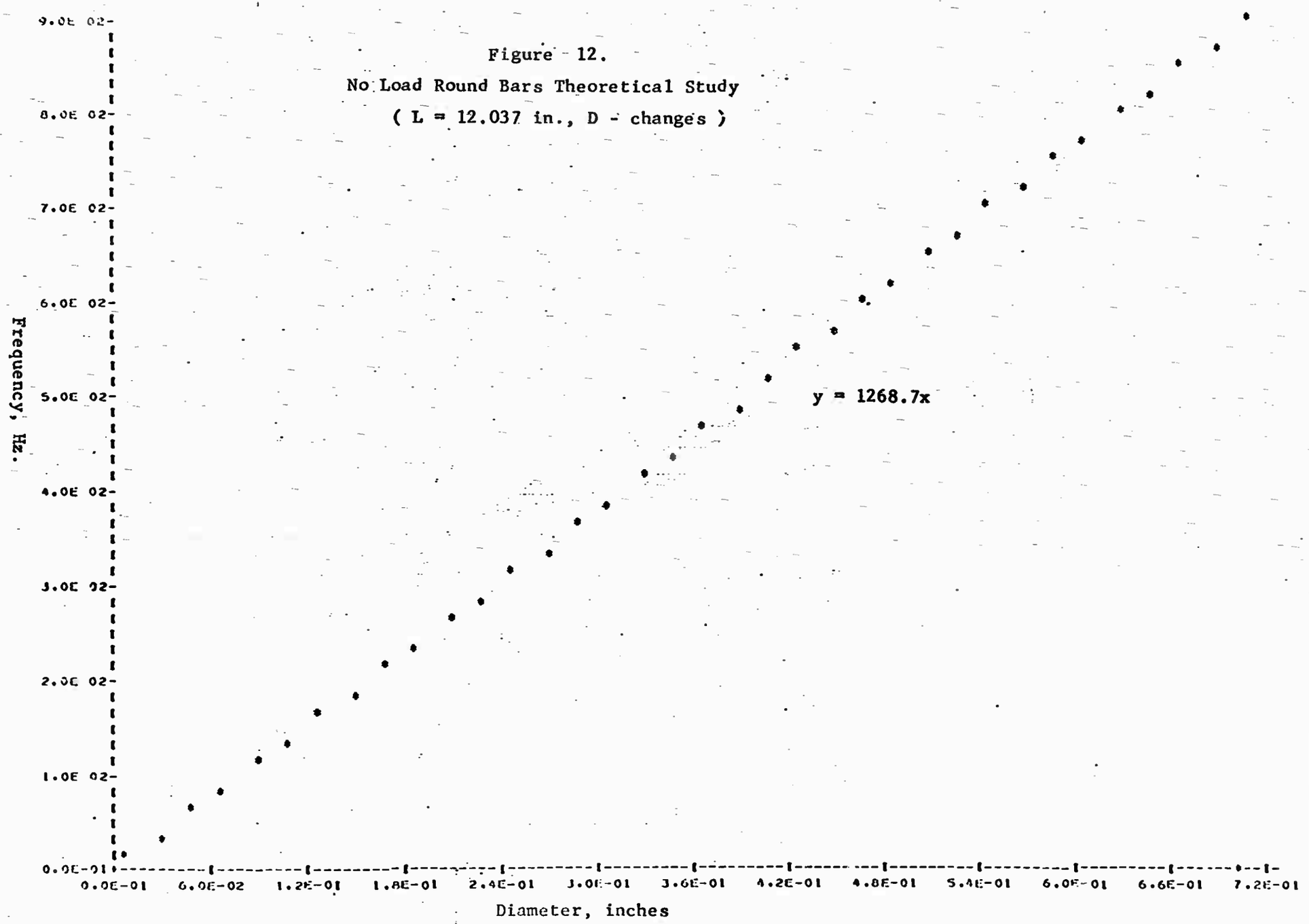

TABLE 11

DIAMETER CHANGE OF ROUND BAR

LENGTH 12.037"

Diameter In	Weight Grams	Frequency, Hz Exp	Theo
.7078	605	898	389
.6995	590	888	385
.6950	585	888	381
.6880	575	894	377
.6860	565	890	378
.6800	553	887	376
.6485	500	848	360
.6250	470	816	344
.6150	455	812	339

Rolled Bars

The 29 rolled bars received from Frankford Arsenal have dimensions of approximately ¼ x 2 x 5½ inches. They have varying hardness ranging from 92.5 to 95 on the Rockwell "B" scale.

The experimental set up was consistent in that a sytrofoam support apparatus was used and the bars were struck with the solenoid used in previous experiments. The variability of the resulting frequencies were so small that no difference could be recognized although there was a slight varying in hardness. One bar, however, gave a frequency of 2 resolution width below the others. It was x-rayed with an average bar of the medium hardness of the range group but no flaws was detected in either bar. Further examination showed that the bar that gave the lower frequency was longer than any other bars by 0.1406 inches. According to the theoretical equation, length is inversely proportional to frequency, which would tend to explain the lower frequency.

Thin Wall, Metal Tubing

Two 0.230 inch OD, stainless steel tubes, four feet long were received to be tested. They were sent by WADCO (a subsidiary of Westinghouse Electric Corporation) in Richland, Washington.

The purpose of the test was to obtain an audio range envelope by striking the tubes at different points along the tube to ascertain any difference in frequency that could be attributable to some defect in the tube.

Many different configurations were tried, two of which are shown in Figures 13 and 14. In Figure 13, the tube was simply supported at its ends by two pencils as shown. It was then excited at the three positions A, B, and C. The envelope was recorded and played back to the hybrid computer. The results are shown below the figure.

In Figure 14, a second position was set up with the tube being supported in a sound box is shown. Response was recorded by striking the tube at points a, b, c and d. The sound was then played back to the computer with the results as shown in the figure.

Obtaining an envelope from the tube was difficult because of the small mass and the inherent flexibility of the tube. However, the vertical configuration (Figure 14) shows promise because of the amplifying power of the sound box. If further investigation could be made, a more precise analysis of the tubes might be obtained.

In summary, further investigations appear worth pursuing but since the data collecting configuration is constructed for machine parts of some mass, it will have to be altered to obtain satisfactory response from light mass tubing.

Sensitivity to a Small Hole

To determine the sensitivity of the acoustical technique to discontinuities a 1/60 inch hole was drilled thru the center diameter axis of a round carbon steel bar. The bar was tested before and after drilling in the usual manner.

The first run to ascertain the effect of the 1/60" drilled hole through the center axis of the round carbon steel bar was not successful. The bar had a diameter of 0.70 inch. The frequency of the bar before the hole was drilled was within the interval of 982 - 986 Hz which is within the minimum frequency resolution. The frequency after the hole was drilled remained within the 982 - 986 Hz interval. One hypothesized reason was that the undrilled bar had a frequency of 986 Hz and after drilling the frequency was only as low as 982 Hz. This is one of the fallacies of the technique, but the probability of this occurring regularly is not great.

The second run was more successful. The diameter of the bar was 0.50 inch. The frequency before drilling the 1/60" hole was approximately 656 Hz. After the hole was drilled the frequency dropped to approximately 640 cps. Note the difference in diameter.

Since the theoretical model agrees extremely well with the experimental findings, the system can now predict the frequency change due to the dimensional changes. As a result, the dimensional changes in the stress experiment can now be separated from the overall frequency changes. That is, the frequency change due to stress alone can be isolated.

The frequency change due to the dimensional change can be derived from the theoretical equations. The relations between the frequency and the length or diameter are

$$f \sim 1/L^2 \text{ or } f \sim D^2$$

Taking a derivative of the above equation and dividing the derivations by the original equations:

$$\frac{df}{f} = -2\,\frac{dL}{L} \quad \text{and} \quad \frac{df}{f} = 2\,\frac{dD}{D}$$

If there is a one percent change in length ($dL/L = 1\%$) or in diameter ($dD/D = 1\%$) a two percent change in frequency will result. Since the frequency change due to the dimensional change is isolated, the stress and frequency relation is established. (The minus sign means an increase in length results a decrease in frequency).

Conclusions--Phase III

Perhaps the most exciting and unexpected results of this research was the high degree of sensitivity of the system to detect differences in stresses in machine elements. From this it might be concluded that the possibility might exists for determining the degree of stress in machine elements, in situ. Elements, such as pins, connecting rods, shafts, and linkages, could be tested without being removed from the system and any unusual degree of stress in those members could be ascertained. Applications of this type of nondestructive test could apply to such diverse systems as internal combustion engines, transmission towers, bridges, and airframes.

As was anticipated, the system had the ability to determine changes in dimensional lengths and diameters of the order of magnitude sufficiently small to consider the process here developed as an inspection tool.

For many years the control of liquids and gases has been a process which could easily be automated. The automated control of hardware is in the infant stage in that the development of airgages and other automated inspection tools are new. The system developed here could add to the small number of devices now available to automatically inspect machine elements or any other matallic element where some dimensional

property is of interest. In addition, where it is of interest to determine significant deterioration, it is possible to apply the nondestructive test to determine whether the element is in the essentially original configuration.

The rolled sections received from Frankford Arsenal presented a rather unusual situation. These items of steel were rolled in such a manner that the configuration was not necessarily uniform. The system had the ability to choose one of 29 bars which was significantly different in configuration from the others. Since the bar was significantly different (on the order of magnitude of 0.25 inches), the sensitivity of the system to rolled elements remains to be ascertained. If the system proves applicable to this type of test, then the whole field of consideration of unusual size and shape castings might be amenable to this type of nondestructive test.

It is considered that the sample size used for the long, thin walled tubing was too small to draw any meaningful conclusions. It is recognized that there are mounting and damping problems which tend to make the energy envelope, received from vibrating this type of configuration, difficult to retrieve. Nevertheless, there appears to be no real barrier to developing a computerized nondestructive testing technique for these types of tubes.

Again, as anticipated, the drilling of a 1/60 inch round hole in a machine bar gave a sufficiently different response frequency so that any anticipated nondestructive computerized test to pickup faults as big as 1/60 inch is feasible. Additional work will be necessary to refine the tests for smaller faults.

Recommendations--Entire Study

Since nearly all of the tests considered here appear to be feasible it is recommended that additional work within each area, i.e., stress, dimensional differences, and structural integrity be investigated further. Standards for mounting specimens must be developed and background frequency responses for standard pieces must be ascertained.

The sensitivity of all of the tests remains to be investigated.

It is believed by the researchers that a small portable computer can be developed to conduct the tests described here. This would require the joint effort of those interested in nondestructive testing and those knowledgable about computer and circuit design.

In summary, the overall conclusion from this research indicates that the computer will assume an increasing role in nondestructive testing and that the computer does, indeed, have the ability to store and compare data so that it can be a decision making tool.

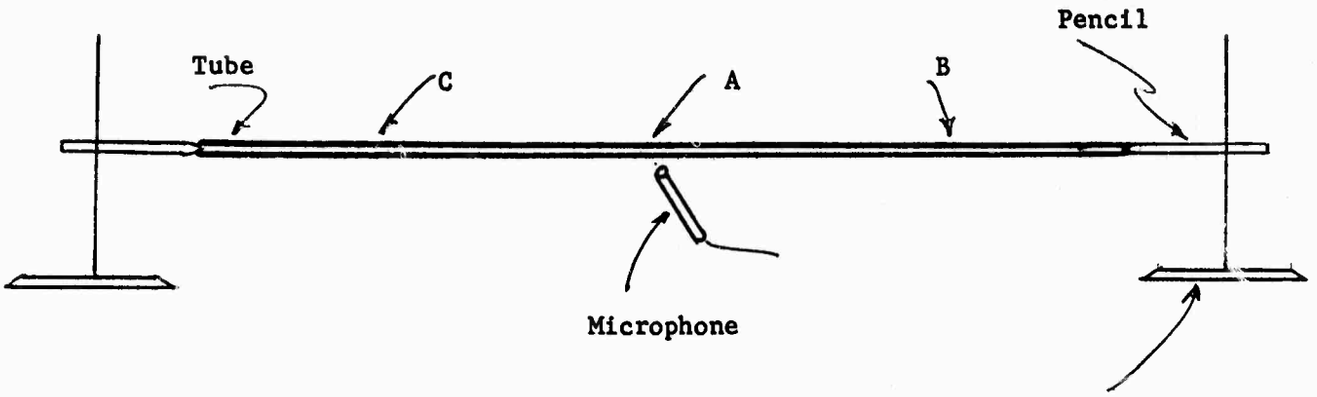

FREQUENCY	POSITION		
Tube	A	B	C
NDT6	856	856	1984
007	812	---	----

FIGURE 13

HORIZONTAL TEST CONFIGURATION FOR THIN WALL TUBING

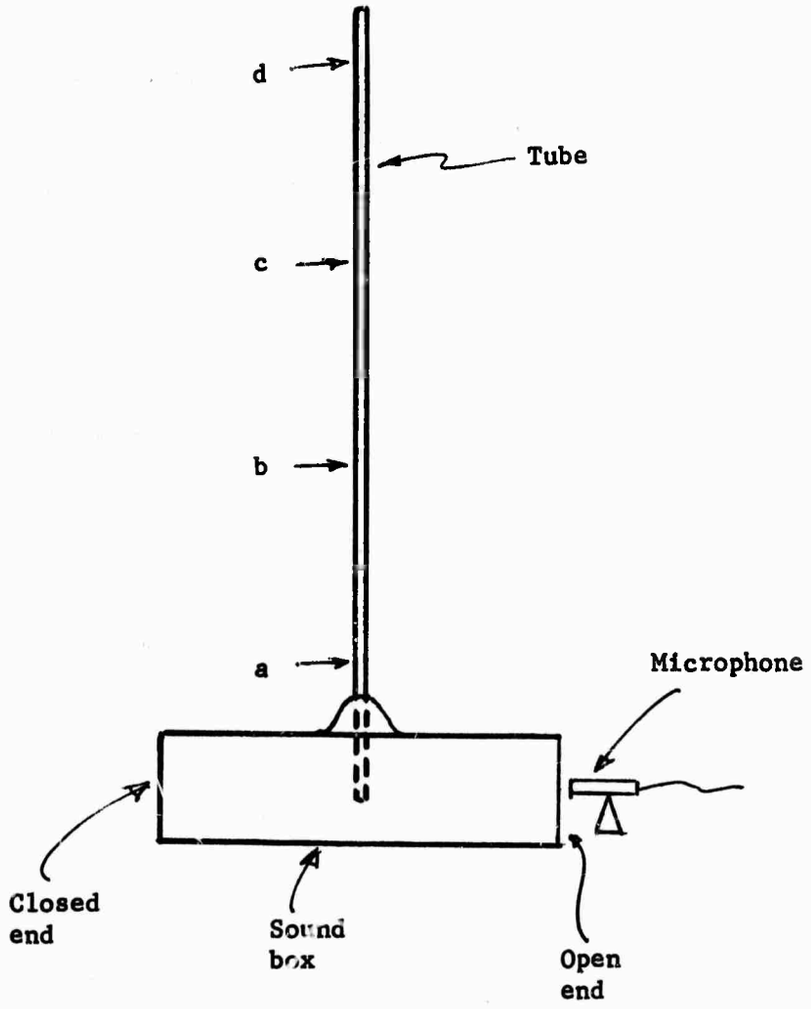

	NDT6		007	
	1	2	1	2
a	316	437	199	199
b	589	582	558	558
c	589	585	562	562
d	593	585	---	558

FIGURE 14

VERTICAL TEST CONFIGURATION FOR THIN WALL TUBING

LIST OF REFERENCES

1. Bendat, J. S. and A. G. Piersol, Measurement and Analysis of Random Data, John Wiley and Sons, Inc., 1966.

2. Brenner, Norman, "Three FORTRAN Programs that Perform the Cooley-Tukey Fourier Transform", Tech. Note 1967-2 MIT Lincoln Lab., July 1967.

3. Cooley, J. W. and J. W. Tukey, "An Algorithm for Machine Calculation of Complex Fourier Series", Mathematics of Computers, Vol. 19, pp. 297-301, April 1965.

4. Cooper, G. R. and C. D. McGillem, Methods of Signal and System Analysis, Holt, Rinehart and Winston, Inc., N. Y., 1967, Chapters 5, 6, 10 and 11.

5. General Electric Company Technical Report, Contract DA-36-038-AMC-1855(A) for Frankford Arsenal, "Engine Vibration Diagnostic Program for Automatic Checkout System for Combat Vehicles", June 1966.

6. Lee, Y. W., Statistical Theory of Communication, John Wiley and Sons, Inc., New York, 1960.

7. Mix, D. F., Random Signal Analysis, Addison-Wesley Publishing Co., Reading, Mass., 1969, Chapters 2, 3 and 10.

8. Peterson, A P. and E. E. Gross, Jr., Handbook of Noise Measurement, (Sixth Edition), General Radio Co., West Concord, Mass.

9. Redwood, Martin, Mechanical Waveguides, Pergamon Press, 1960.

10. Rothman, James E., "The Fast Fourier Transform and its Implementation", Decuscope, Vol. 7, No. 3, 1968.

11. Stacy, Ralph W. and B. D. Waxman, Computers in Biomedical Research, Vol. II, Academic Press, 1965.

APPENDIX A

ANALYSIS THEORY AND DATA REDUCTION

The data gathered from striking a bar are primarily of a transient type with superimposed resonance modes and some random noises. The factors that contribute to the shape of the energy envelope might very well be involved with the way the bar is struck, the bar size, the bar material and the manner in which the system is mounted. Two approaches seem to offer the most promise in analyzing this type of data. The direct approach is the comparison of the raw data of the defective sample and a standard. Another approach is the comparison of the data in their frequency domain, which is obtained by a transform of the raw data. The second approach was chosen for the following reasons: 1) The comparison in the frequency domain is a shorter one, especially when data records are long. 2) The amplitudes in the frequency domain are sensitive. It is anticipated that resonance peaks could provide easily identifiable features in order to distinguish the defective samples when their frequency or amplitudes deviated from that of the standard sample. It is expected that a resonant frequency will be associated with each sample and that it can be readily identified. 3) Finally, the frequency analysis is a well known and tested method and the statistical tools are readily available.

The transformation from the time-history-records, x(t), to their frequency representation, F(f), is generally done by the Fourier transform

$$F(f) = \int_{-\infty}^{\infty} x(t)\, \exp(-2\pi i f t)\, dt.$$

Where i is $\sqrt{-1}$. A faster version of the transform has been developed in recent years. It was known as the Cooley and Tukey Fast Fourier Transform. The analysis program developed for this research project has adapted a Fast Fourier Transform Subroutine through IBM contributed program library (subroutine FOUR1). This subroutine performs a discrete Fourier transform of a set of N equally spaced, time samples, x_o, x_1, ..., x_{N-1} and is given by

$$F_k = \sum_{J=0}^{N-1} x_j \exp(-2\pi i j/N),\ k = 0,1,\ldots,N.$$

To compute the frequency spectrum F_k, would normally require N^2 complex multiplications. However, a reduction in operations can be achieved if N is a power of 2. An algorithm developed by Cooley and Tukey[3], called the Fast Fourier Transform, performs the same transform in $N(\log_2 N)$ complex multiplications, thus reduces the computing time by approximately 99%[7].

Mathematically speaking, the transformed values, F_k, are the coefficients of the Fourier series which may be either negative, positive, or zero. It was found more expedient to compare the power spectral density function, that is, the mean square value, rather than the frequency spectrum. Apparently the time series data was not probabilistic in nature, but using the average squared values has the advantage of emphasizing the peaks and de-emphasizing the minor features. For this reason the power spectral density function, $G_x(f)$, were calculated which were obtained by filtering the sample-time-history record in a frequency range from f to $(f + \Delta f)$, squaring them and averaging the squared output from the filter. Mathematically, the power spectral density function is defined as[1]

$$G_x(f) = \lim_{\Delta f \to 0} \lim_{T \to \infty} \frac{1}{(\Delta f)T} \int_0^T x^2(t,f,\Delta f)\, dt,$$

where T is the total record time. For stationary data[1], the power spectral density function is related to the auto-correlation function by the Fourier transform

$$G_x(f) = 2 \int_{-\infty}^{\infty} R_x(\tau) \exp(-2\pi i f \tau)\, d\tau,$$

where $R_x(\tau)$ is the auto-correlation function which describes the dependence of the sample-time-history records, $x(t)$ and $x(t + \tau)$, and τ is the time lag between the two records. It is defined mathematically as an average over the observation time, T, and is the real-valued function,

$$R_x(\tau) = \lim_{T \to \infty} \frac{1}{T} \int_0^T x(t)\, x(t+\tau)\, dt.$$

Note that when $\tau = 0$, the auto-correlation function is the mean square value and has reached a maximum. In physically realizable situations, only one-sided power density functions can be obtained, where frequency, f, varies from 0 to ∞. That means $R_x(\tau)$ should be treated as an even function of τ, and the spectral density function is equivalent to folding over the negative terms from the Fourier transform into the positive direction.

$$G_x(f) = 4 \int_0^{\infty} R_x(\tau) \cos 2\pi f\tau d\tau$$

A convenient way to make a comparison between bars is that of using the cross spectral functions. A computer program has been written to cross-correlate the data between bars. Test cases have been tried on the program. The cross-correlation function is a function which describes the mathematical dependence of the time history records similar to the auto-correlation function except that the correlations are between two different sets of data. It can be expressed as

$$R_{xy}(\tau) = \lim_{T \to \infty} \frac{1}{T} \int_0^T x(t)y(t + \tau)\, dt,$$

which is a real-valued function but does not necessarily have a maximum when $\tau = 0$, nor is it an even function. The cross-spectral density function, $G_{xy}(f)$, is obtained by the Fourier transform of the cross-correlation function $R_{xy}(\tau)$. It is done in a similar manner as the auto-correlation function is transformed into the power spectral density function. However, the cross-correlation function is not an even function, the resulting cross-spectrum of the Fourier Transform has the complex form

$$G_{xy}(f) = C_{xy}(f) - iQ_{xy}(f),$$

where $C_{xy}(f)$ is the co-spectral density function, which is defined as

$$C_{xy}(f) = \lim_{\Delta f \to 0} \lim_{T \to \infty} \frac{1}{(\Delta f)T} \int_0^T x(t,f,\Delta f)y(t,f.\Delta f)\, dt.$$

It represents the average product of x(t) and y(t) within a narrow frequency interval between f and $(f + \Delta f)$, divided by the frequency interval. The frequency $Q_{xy}(f)$, is called the quandrature spectral density function. It is the imaginary part of the transformed result and is defined as

$$Q_{xy}(f) = \lim_{\Delta f \to 0} \lim_{T \to \infty} \frac{1}{(\Delta f)T} \int_0^T x(t,f,\Delta f)y^*(t,f,\Delta f)\, dt,$$

where $y^*(t,f,\Delta f)$ represents the time shifted $y(t)$, within the frequency internal f and $(f + \Delta f)$, which results in 90 degree phase shift in the complex plane. The actual computations of C_{xy} and Q_{xy} are obtained from the transform of the even and odd parts of the cross-correlation functions, denoted by A_{xy} and B_{xy}, respectively.

$$A_{xy}(f) = \frac{1}{2}\left[R_{xy}(f) + R_{yx}(f)\right]$$

$$B_{xy}(f) = \frac{1}{2}\left[R_{xy}(f) - R_{yx}(f)\right]$$

The co-spectral density function is the Fourier transform of A_{xy} and the quandrative spectral density function is the Fourier transform of B_{xy}. The magnitude of the cross spectral density function is

$$G_{xy}(f) = C^2_{xy}(f) + Q^2_{xy}(f),$$

and the phase angle is

$$\theta_{xy}(f) = \tan^{-1}[Q_{xy}(f)/C_{xy}(f)].$$

The comparison between the two history records can be assessed by the cross and auto-spectral density functions. The combined function is called the coherent function and is defined as

$$\gamma^2_{xy}(f) = \frac{G^2_{xy}(f)}{G_x(f)G_y(f)} \leq 1,$$

which varies between 0 and 1. $\gamma^2_{xy}(f) = 0$, indicates incoherent and the value, $\gamma^2_{xy}(f) = 1$, indicates fully coherent. If two bars have a perfect match the coherent function should be 1 at all frequencies. When there are deviations between bars, the coherence function drops off a frequencies where power spectra are out of agreement.

APPENDIX B

PROGRAMMING AND THEORY

During the initial part of the program use was made of a digital computer (IBM 360, Model 65) entirely. Then analysis was done on a hybrid computer of sufficient capacity to analyze any data which may be encountered in this project. The hybrid system in question uses a Sigma 5 for the digital components and EAI 680 for the analog component.

Since hybrid computers are relatively new items of equipment it may be well here to mention some advantages and disadvantages of analog, digital and hybrid computers.

The analog computation has the disadvantage of having a limited precision of one part in one thousand. Another disadvantage lies in the necessity to increase the size of the computer capacity directly with the problem size. Further it is necessary to establish a program by inner connecting computer elements with wires and the reliability limitations inherent in linear devices (as compared to discrete devices).

The digital computer, on the other hand, is a very high precision piece of equipment with nearly absolute repeatability. Further, digital programs can be escaladed in complication, a piece at a time, and changing from one program to another is simple. Another attractive feature of the digital computer lies in its ability to handle logical, Boolean and algebraic operations and to react to inputs that send it on completely different courses of action, such as interrupts.

Of course, the digital computer has its disadvantages, the first being it is a slow integrating device. In addition, man-machine interface continues to be a time consuming problem. Finally, cost are very great in digital equipment.

The main advantage of the analog computer lies in its ability to receive voltage equivalent signals and deal with these directly, whereas the information must be digitized to employ a digital computer.

The hybrid computer simply combines the integrating speed of the analog and the accuracy, arithmetic and logical operation of the digital so that problems done either poorly or not at all by either analog or digital machines can be solved.

For the particular application of hybrid computer to the investigation in question the analog to digital converter and the digital part of the computer allow the on-line, real-time analysis of the data so that information can be obtained immediately.

The sound signature analysis is usually done by converting the time series data into their frequency domain by a direct Fourier intergal transformation of the data. The resulting frequency spectrum describes the frequency response of the sounding system. The frequency representation of a sound signature reveals much of the physical characteristics of the sounding source. When the relative power representation of the sound signature is described as a function of frequency, a power spectral density function is obtained indirectly by the Fourier transform of its autocorrelation function. The distinction between the power spectrum and the direct Fourier transformed spectrum from the sound signature is similar to the comparison of a sine-squared function to a sine function. The natural frequency is greatly magnified and the noise frequencies are relatively depressed in the power spectral representation. No negative values should be found in the power spectrum theoretically (although digitized formulation sometimes produces a slight negative spike). The reason that the power spectral analysis is favored lies in the ascertaining of whether a minute change in the specimen can cause corresponding change in the magnified response frequency peak of the power spectrum.

To illustrate the direct Fourier transform of a time series data x(t), let F(f) represent their transformed value in the frequency domain.

$$F(f) = \int_{-\infty}^{\infty} x(t) \cdot e^{-2\pi i f t} dt$$

where f is the frequency variable, i is equal to $\sqrt{-1}$, and t is the time variable. If x(t) is a single rectangular pulse, see Figure 15, the corresponding frequency spectrum is shown in Figure 16.

Its power spectrum representative is shown in Figure 17.

If x(t) is a pure sine function, its corresponding frequency representation is shown in Figures 18 & 19. The sound signature in the heat-treated bar experiments were sinusoidal waves superimposed with an exponential damping, with some low frequency components and high frequency noise. The recorded sound data were first digitized by either a CAT computer or hybrid system. Its autocorrelation function was determined by the relation,

FIGURE 15

SQUARE PULSE-INPUT SPECTRUM

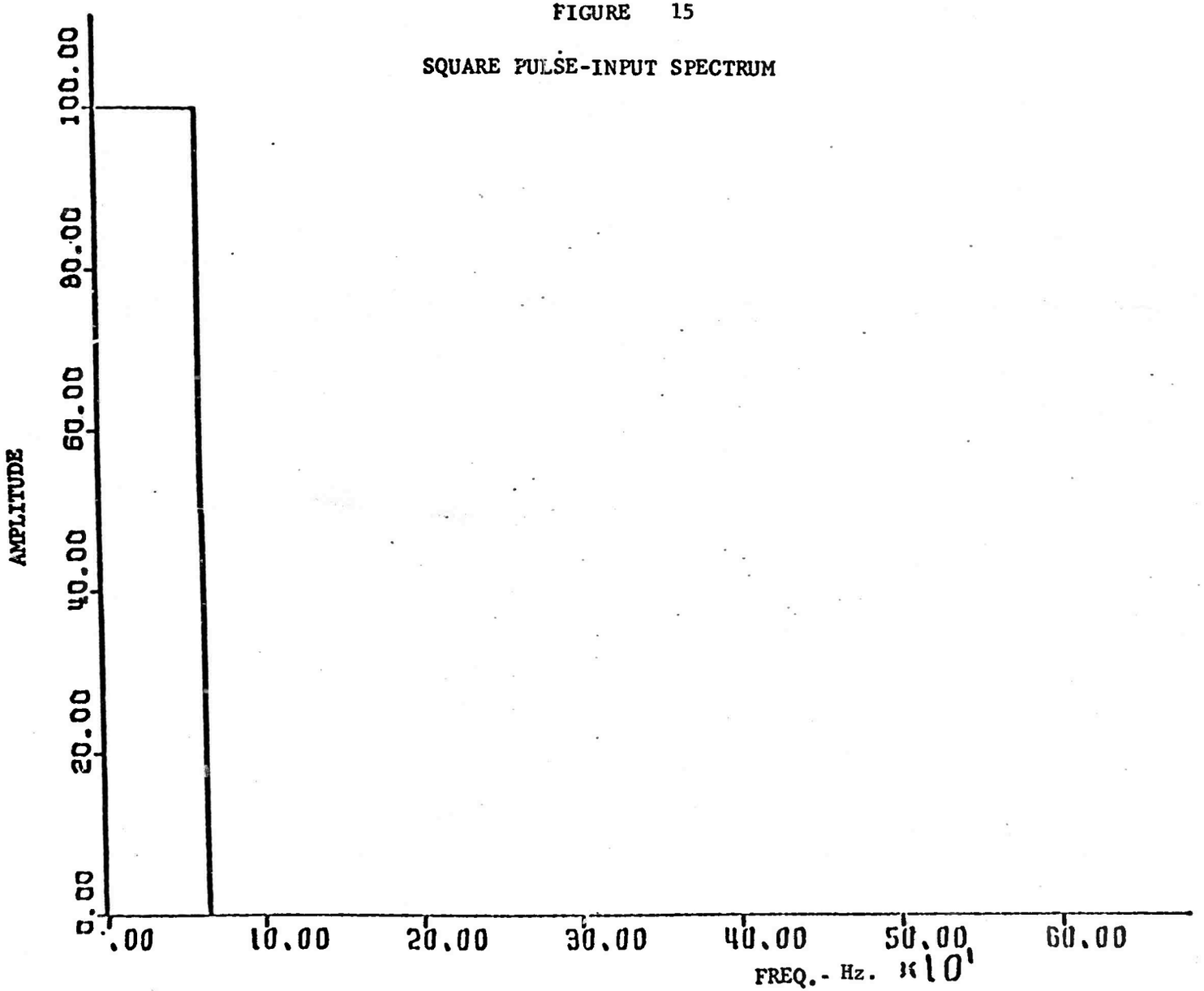

FIGURE 16

SQUARE PULSE-FREQ. SPECTRUM

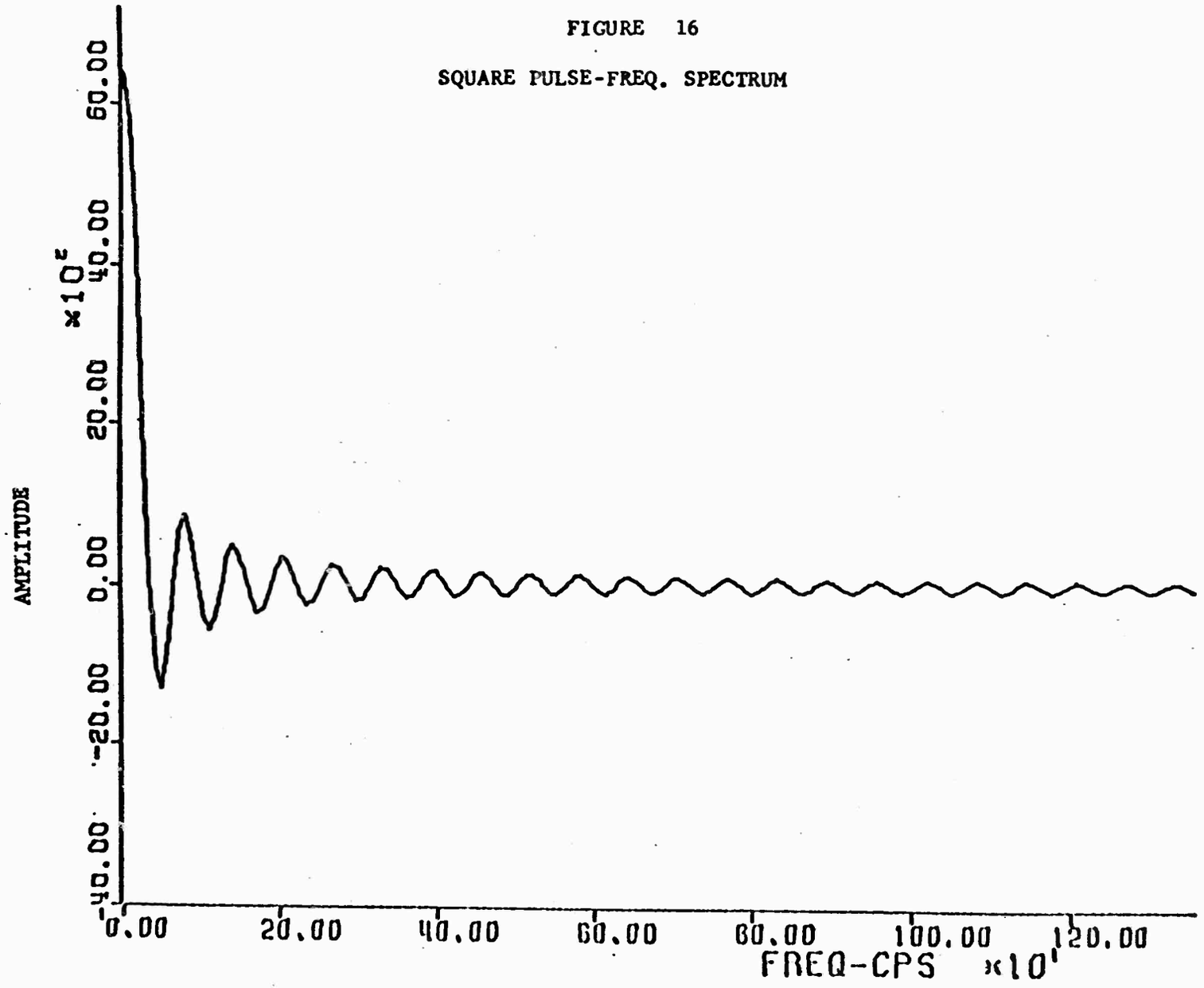

FIGURE 17

SQUARE PULSE-POWER SPECTRUM

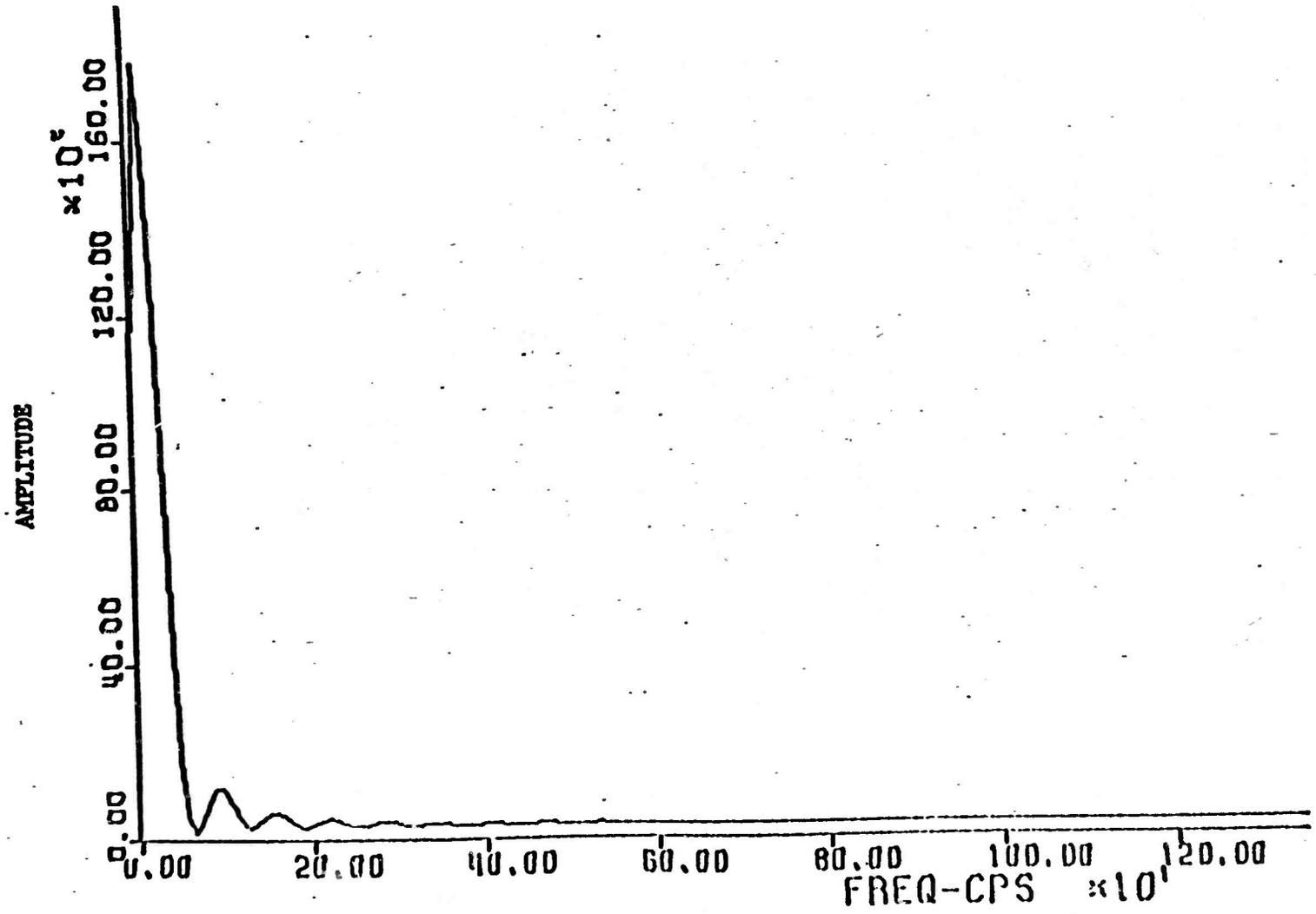

FIGURE 18

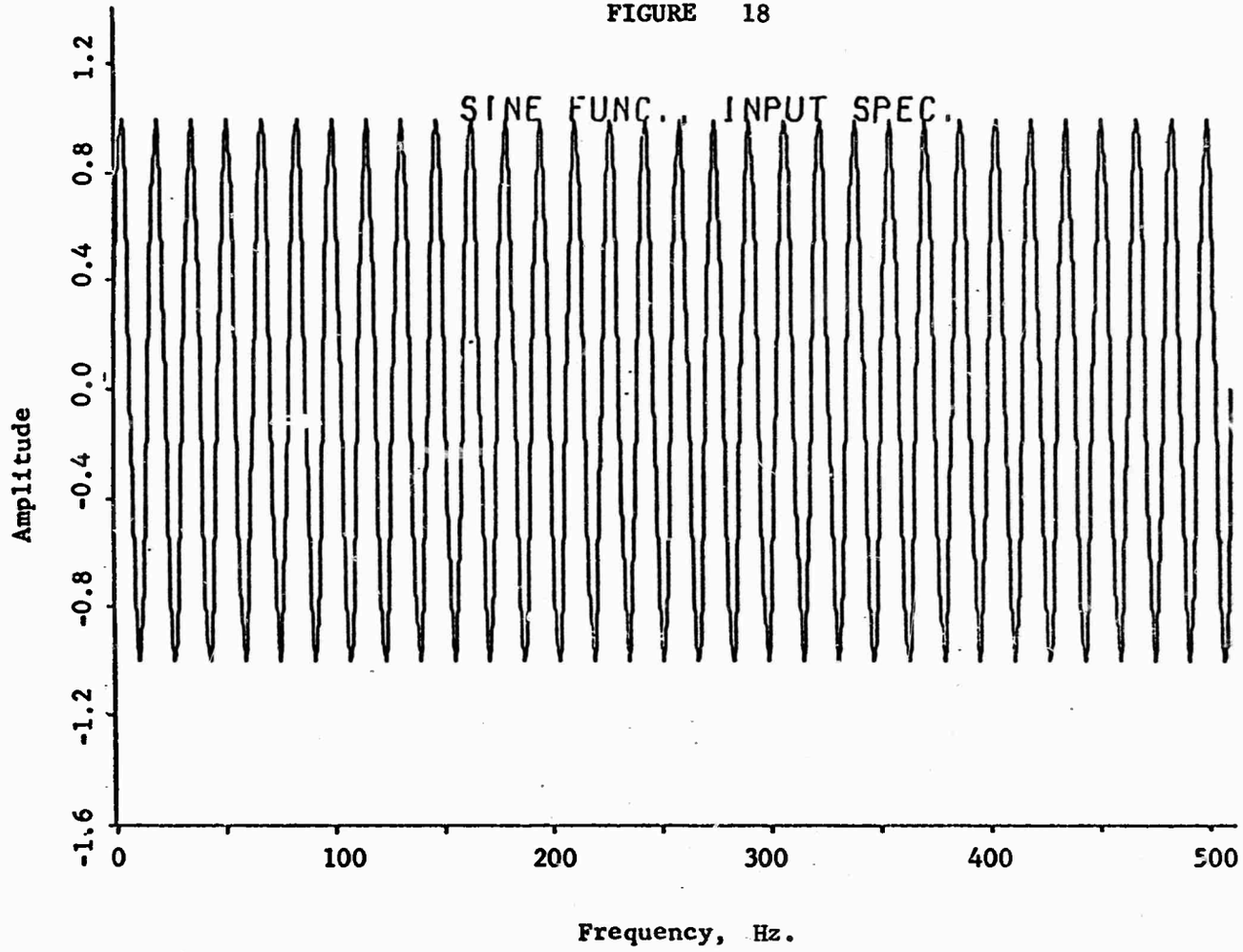
SINE FUNC., INPUT SPEC.
Amplitude
1.2
0.8
0.4
0.0
-0.4
-0.8
-1.2
-1.6
0
100
200
300
400
500
Frequency, Hz.

FIGURE 19

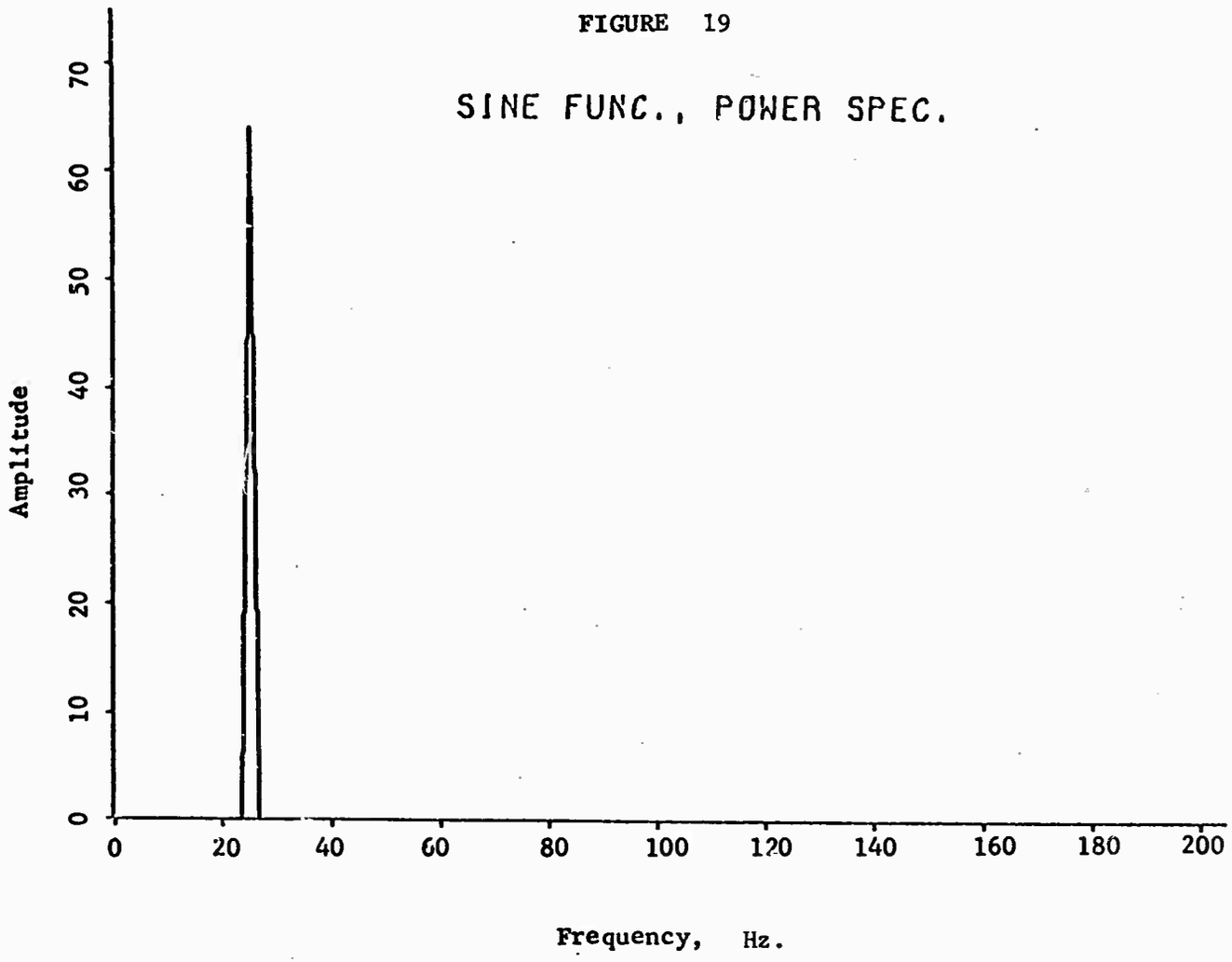
SINE FUNC., POWER SPEC.
Amplitude
0
10
20
30
40
50
60
70
0
20
40
60
80
100
120
140
160
180
200
Frequency, Hz.

$$R(\tau) = \frac{1}{T}\int_0^T x(t)\, x(t+\tau)\, dt,$$

where τ represents the time lag between the sampling points and T is the total sample record length in time. The time lag, τ, is a variable ranging from 0 to the maximum lag, L. To get a small statistical uncertainty choose small L, such that $L \ll T$. But in order to have high frequency resolution choose a larger L, such that $L < T$. A compromise choice was used in the sound data analysis such that $L/T = \frac{1}{4}$ to $\frac{1}{2}$ where T represents 1024 sampling points.

The time interval between sampling points could be selected using the CAT unit. The most frequently used time interval was 0.25 millisec. This would give a Nyquist frequency f_c (cut off frequency) of

$$f_c = \frac{1}{2h} = \frac{1000}{2x.25} = 2000 \text{ Hertz}$$

where h is the time interval in seconds.

For the hybrid system, the time interval between points is controlled by a digitizing circuit. The perferred interval is 0.2 millisec, which gives a Nyquist frequency of 2500 Hertz.

After the digitized information was obtained, it was transferred and stored in the memory core of the digital computer. The autocorrelation function $R(\ell)$ is then calculated by the digitized formula

$$R(\ell) = \frac{1}{N-\ell}\sum_{n-1}^{N-\ell} x_n x_{n+\ell} \qquad \ell = 0,1,2,\ldots L$$

where ℓ is the lag number, L is the maximum lag number and $R(\ell)$ is the autocorrelation function at lag ℓ. The equivalent bandwidth of the computational procedure is

$$B = \frac{2f_c}{L} = \frac{1}{Lh}$$

where the equivalent bandwidth B is twice the range found by dividing the frequency interval $(0, f_c)$ into L equally spaced parts, or f_c/L parts.

The autocorrelation function may take on negative as well as positive values. When $\ell = 0$, the autocorrelation function is

$$R_o = R(0) = \frac{1}{N} \sum_{n=1}^{N} (x_n)^2 = \overline{x}^2$$

where x_n are the digitized zero-mean time series data. R_o is related to the sample variance s^2 by the relation

$$R_o = \left(\frac{N-1}{N}\right) s^2$$

The power spectral density function, G(f), is calculated by means of a fast Fourier transform algorithm developed by Cooley and Tukey, which reduces a L^2 complex multiplications to only $L \log_2 L$ complex multiples if the max lag L is an integer power of 2. This reduces the computation time by as much as 99%. The definition of power spectral density function is given in Appendix A. However, for continuity of discussion, some repetition will be done here. G(f) is always a real-valued, non-negative function. By definition

$$G(f) = \lim_{\Delta f \to 0} \lim_{T \to \infty} \frac{1}{(\Delta f)T} \int_o^T x^2(t,f,\Delta f)\, dt$$

where $x(t,f,\Delta f)$ is that portion of x(t) in the frequency range from f to $(f+\Delta f)$. For stationary data, the power spectral density function and the autocorrelation function is related by a Fourier transform as follows:

$$G(f) = 2\int_{-\infty}^{\infty} R(\tau) e^{-2\pi i f}\, d\tau$$

Since $R(\tau)$ is an even function of τ, its digital relation reduces to

$$G_k = 4h \sum_{\ell=0}^{L-1} R_\ell W^{k\ell}, \qquad k = 0,1,\ldots,L-1.$$

where $W = e^{-2\pi i/L}$, L is the max lag, R_ℓ is the digitized autocorrelation function and G_k is the digitized power spectrum.

APPENDIX C

Stressed Bar Model Theory

Applying d'Alambert's principle to a free lateral vibration of a simply supported bar we have:

$$EI \frac{\partial^4 y}{\partial x^4} - S \frac{\partial^2 y}{\partial x^2} = - \rho \frac{\partial^2 y}{\partial t^2}$$

where E = Young's modulus (psi)

I = moment of inertia of cross section area (in^4)

ρ = linear density (slug/in)

S = applied force (#)

t = time (sec)

Boundary conditions: $y(L,t) = 0$

$y(0,t) = 0$

Proposed solution:

$$y = \sum_{n=0}^{\infty} A_n(t) \operatorname{Sin} \frac{n\pi x}{L} + \sum_{n=0}^{\infty} B_n(t) \operatorname{Cos} \frac{n\pi x}{L}$$

$B_n(t) = 0$ due to the boundary condition

$$\frac{\partial^4 y}{\partial x^4} = \sum_{n=0}^{\infty} \frac{n^4 \pi^4}{L^4} A_n(t) \operatorname{Sin} \frac{n\pi x}{L}$$

$$\frac{\partial^2 y}{\partial x^2} = - \sum_{n=0}^{\infty} \frac{n^2 \pi^2}{L^2} A_n(t) \operatorname{Sin} \frac{n\pi x}{L}$$

$$\frac{\partial^2 y}{\partial t^2} = \sum_{n=0}^{\infty} A_n(t) \operatorname{Sin} \frac{n\pi x}{L}$$

Substituting back into Equation (2)

$$\sum_{n=0}^{\infty} EI \frac{n^4\pi^4}{L^4} A_n(t) \operatorname{Sin} \frac{n\pi x}{L} + \sum_{n=0}^{\infty} S \frac{n^2\pi^2}{L^2} A_n(t) \operatorname{Sin} \frac{n\pi x}{L} =$$

$$-\sum_{n=0}^{\infty} \rho A_n(t) \operatorname{Sin} \frac{n\pi x}{L}$$

The eigen equation is then:

$$EI \frac{n^4\pi^4}{L^4} A_n(t) + S \frac{n^2\pi^2}{L^2} A_n(t) + \rho A_n(t) = 0$$

or, simply a wave equation

$$A_n(t) + \left[\frac{1}{\rho} \left(EI \frac{n^2\pi^2}{L^2} + S \right) \frac{n^2\pi^2}{L^2} \right] A_n(t) = 0$$

The solution of the wave equation is

$$A_n(t) = C_n \operatorname{Sin} \omega t + D_n \operatorname{Cos} \omega t$$

with arbitrary coefficients C_n and D_n.

The corresponding frequency is

$$\omega = \frac{n\pi}{L}\sqrt{\frac{1}{\rho}\left(EI\frac{n^2\pi^2}{L^2} + S\right)}$$

or, the response frequency is:

$$f = \frac{\omega}{2\pi} = \frac{n}{2L}\sqrt{\frac{1}{\rho}\left(EI\frac{n^2\pi^2}{L^2} + S\right)}$$

APPENDIX D

1040 Stressed Bar Data

Load lb	Depth in	Width in	Length in	Frequency, Hz Exp	Theo	
1000	.2534	.9994	11.990	242	175	Bar #1
2000	.2534	.9994	11.993	367	197	
3000	.2534	.9994	11.999	382	216	
4000	.2534	.9994	12.002	398	234	
5000	.2533	.9994	12.005	414	251	
6000	.2533	.9994	12.007	429	266	
7000	.2533	.9994	12.010	---	281	
8000	.2533	.9994	12.012	453	295	
9000	.2532	.9994	12.015	---	309	
10000	.2532	.9994	12.017	---	321	
1000	.2528	1.001	12.340	351	164	Bar #2
2000	.2528	1.001	12.342	351	191	
3000	.2528	1.001	12.344	375	210	
4000	.2528	1.001	12.347	332	228	
5000	.2528	1.001	12.352	398	245	
6000	.2528	1.001	12.357	414	260	
6900	.2527	1.001	12.362	988	273	
8000	.2527	1.001	12.365	960	289	
8900	.2526	1.001	12.368	945	301	
10000	.2526	1.001	12.371	930	315	

	Inches	
Bar	A	B
1	.811	.965
2	.692	.718

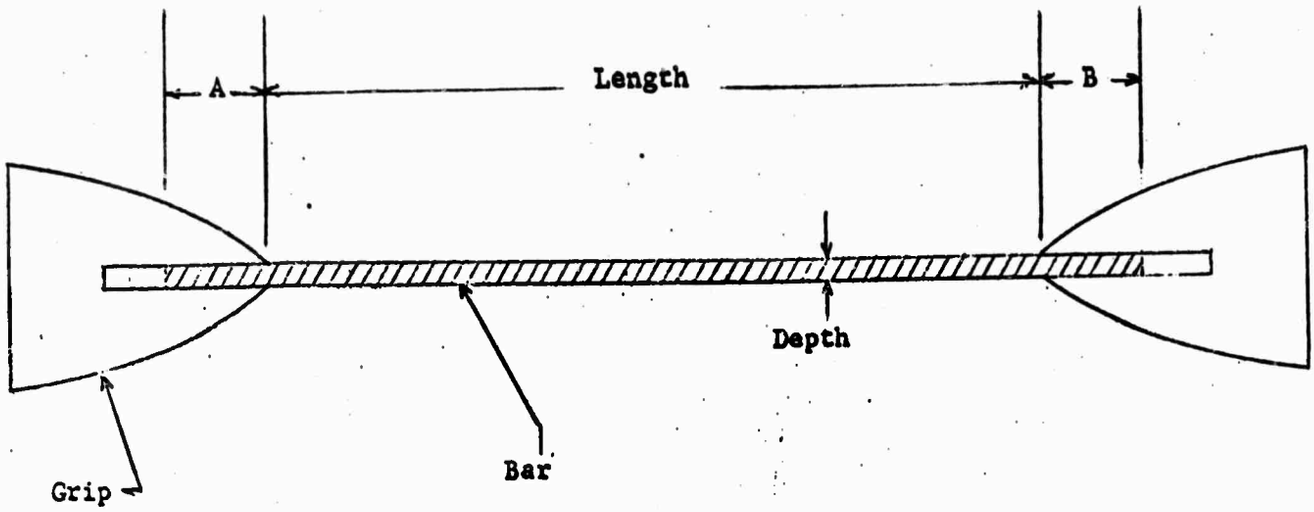

Labels A and B indicate the length of the bar was used for the gripping. These values will be given below each remaining group of tables.

Load lb	Depth in	Width in	Length in	Frequency, Hz Exp	Theo	
1000	.2534	1.000	12.279	335	170	Bar #3
2100	.2534	1.000	12.285	281	194	
3000	.2534	1.000	12.290	250	212	
4000	.2534	1.000	12.294	226	230	
5000	.2533	1.000	12.298	195	246	
6000	.2533	1.000	12.302	414	261	
7000	.2533	1.000	12.305	429	276	
8000	.2533	1.000	12.309	953	290	
9000	.2532	1.000	12.314	929	303	
10000	.2532	1.000	12.317	---	316	
1000	.2540	.9975	11.952	351	177	Bar #4
2000	.2540	.9975	11.955	375	199	
3000	.2540	.9975	11.958	390	219	
4000	.2539	.9975	11.962	406	236	
5000	.2539	.9975	11.965	414	253	
6000	.2538	.9975	11.969	---	269	
7000	.2538	.9975	11.972	---	284	
7900	.2538	.9975	11.975	---	296	
9000	.2538	.9975	11.980	---	312	
10000	.2538	.9975	11.984	---	324	

	Inches	
Bar	A	B
3	.881	.864
4	.945	1.132

Load lb	Depth in	Width in	Length in	Frequency, Hz Exp	Theo	
1000	.2527	1.020	11.978	343	177	Bar #5
2000	.2527	1.020	11.983	375	199	
3000	.2527	1.020	11.988	390	219	
3900	.2526	1.020	11.993	398	235	
5100	.2526	1.020	11.996	414	255	
6000	.2526	1.020	12.000	429	269	
7000	.2526	1.020	12.005	445	283	
8000	.2526	1.020	12.008	921	297	
9000	.2525	1.020	12.011	---	311	
10000	.2525	1.020	12.014	---	324	
1000	.2527	.9998	12.234	335	172	Bar #6
2000	.2527	.9998	12.238	281	194	
3000	.2527	.9998	12.242	375	213	
4000	.2526	.9998	12.247	390	231	
5000	.2526	.9998	12.252	185	248	
6000	.2526	.9998	12.255	414	264	
7000	.2526	.9998	12.258	429	278	
8000	.2526	.9998	12.261	445	292	
9000	.2525	.9998	12.265	453	305	
10000	.2525	.9998	12.271	914	318	

Bar	Inches A	B
5	.956	1.108
6	.780	1.350

Load lb	Depth in	Width in	Length in	Frequency, Hz Exp	Theo	
1000	.2535	1.035	12.180	312	174	Bar #7
2000	.2535	1.035	12.183	265	196	
3000	.2535	1.035	12.189	375	215	
4000	.2534	1.035	12.196	390	232	
5000	.2534	1.035	12.200	406	249	
6000	.2534	1.035	12.205	421	264	
7000	.2534	1.035	12.210	429	279	
7900	.2534	1.035	12.213	445	292	
9000	.2534	1.035	12.217	---	306	
10000	.2533	1.035	12.221	---	319	
1000	.2531	1.005	12.226	320	171	Bar #8
2000	.2531	1.005	12.230	265	193	
3000	.2531	1.005	12.234	382	212	
4000	.2530	1.005	12.238	390	230	
5000	.2530	1.005	12.241	206	247	
6000	.2530	1.005	12.245	421	262	
7000	.2530	1.005	12.248	429	277	
8000	.2529	1.005	12.252	445	291	
9100	.2529	1.005	12.255	---	305	
10000	.2529	1.005	12.260	906	317	

	Inches	
Bar	A	B
7	.860	.970
8	.815	1.020

Load lb	Depth in	Width in	Length in	Frequency, Hz Exp	Theo	
1000	.2535	.9988	12.130	296	174	Bar #9
2000	.2535	.9988	12.134	367	195	
3000	.2535	.9988	12.139	382	215	
4000	.2534	.9988	12.142	398	233	
5000	.2534	.9988	12.147	414	250	
6000	.2534	.9988	12.152	---	265	
7000	.2533	.9988	12.156	437	280	
8000	.2533	.9988	12.158	445	294	
9000	.2533	.9988	12.161	---	308	
10000	.2533	.9988	12.166	898	320	
1000	.2528	.9800	12.123	281	172	Bar #10
2000	.2528	.9800	12.125	367	194	
3000	.2528	.9800	12.128	382	214	
4000	.2527	.9800	12.131	398	232	
5000	.2527	.9800	12.135	406	249	
6000	.2527	.9800	12.139	421	264	
7000	.2526	.9800	12.142	437	279	
8000	.2526	.9800	12.145	937	293	
9000	.2526	.9800	12.150	914	307	
10000	.2526	.9800	12.155	898	320	

	Inches	
Bar	A	B
9	.880	1.150
10	.922	.970

Load lb	Depth in	Width in	Length in	Frequency, Hz Exp	Theo	
1000	.2526	.9945	12.082	281	173	Bar #11
2000	.2526	.9945	12.085	367	195	
3000	.2526	.9945	12.090	382	214	
4000	.2525	.9945	12.095	398	232	
5000	.2525	.9945	12.100	414	249	
6000	.2525	.9945	12.105	421	264	
7000	.2525	.9945	12.109	437	279	
8000	.2524	.9945	12.113	929	293	
9000	.2524	.9945	12.116	910	306	
10000	.2524	.9945	12.020	890	321	
1000	.2535	.9965	12.125	343	173	Bar #12
2000	.2535	.9965	12.130	367	194	
3000	.2535	.9965	12.135	382	214	
4000	.2535	.9965	12.140	398	323	
5000	.2534	.9965	12.144	414	248	
6000	.2534	.9965	12.148	421	264	
7000	.2534	.9965	12.152	437	279	
8000	.2534	.9965	12.155	929	293	
9000	.2534	.9965	12.159	914	306	
10000	.2533	.9965	12.164	890	318	

	Inches	
Bar	A	B
11	.955	1.00
12	.905	1.00

Load lb	Depth in	Width in	Length in	Frequency, Hz Exp	Frequency, Hz Theo	
1000	.2525	1.005	12.120	304	173	Bar #13
2000	.2525	1.005	12.126	367	194	
3000	.2525	1.005	12.131	382	214	
4000	.2525	1.005	12.135	398	232	
5000	.2524	1.005	12.140	414	248	
6000	.2524	1.005	12.143	421	264	
7000	.2524	1.005	12.146	437	279	
8000	.2524	1.005	12.150	929	293	
9000	.2524	1.005	12.155	914	306	
10000	.2524	1.005	12.159	898	319	
1700	.2521	.9958	11.505	375	198	Bar #14
2050	.2521	.9958	11.507	390	206	
3000	.2520	.9958	11.514	405	224	
4000	.2520	.9958	11.520	420	242	
4900	.2520	.9958	11.523	---	257	
6000	.2520	.9958	11.528	452	275	
7000	.2520	.9958	11.532	468	290	
8000	.2520	.9958	11.536	---	304	
9000	.2520	.9958	11.538	684	317	
10000	.2520	.9958	11.540	700	330	

Bar	A	B
13	.818	1.105
14	NA.	NA.

APPENDIX E

Theoretical Model to Develop Frequency of Non-stressed, Simply Supported Bars

Simply Supported Bar Without Stress

The moment equation of a simply supported bar is given as

$$EI \frac{d^2y}{dx^2} = -M$$

If we take the second derivative of the above equation with respect to x, we obtain the shearing force

$$\frac{d^2}{dx^2}\left(EI \frac{d^2y}{dx^2}\right) = F$$

now, applying d'Alembert's principle, the vibrating bar is loaded by inertia forces varying along the length of the bar:

$$-\rho \frac{\partial^2 y}{dt^2}$$

and is balanced by the shearing force

$$EI \frac{\partial^4 y}{\partial x^4} = -\rho \frac{\partial^2 y}{\partial t^2}$$

where E = Young's modulus (psi)

ρ = linear density (slug/in)

y = y(x,t)

I = moment of inertia of cross section area (in^4)

Boundary conditions: $y(L,t) = y(0,t) = 0$

Propose solution: $y = \sum_{n>0}^{\infty} A_n(t) \operatorname{Sin} \frac{n\pi x}{L} + \sum_{n=0}^{\infty} B_n(t) \operatorname{Cos} \frac{n\pi x}{L}$

$B_n(t) = 0$ due to the boundary condition.

$$\therefore \quad y = \sum_{n=0}^{\infty} A_n(t) \operatorname{Sin} \frac{n\pi x}{L} \operatorname{Sin} \frac{n\pi x}{L} ;$$

$$\frac{\partial^2 y}{\partial t^2} = \sum_{n=0}^{\infty} \ddot{A}_n(t) \operatorname{Sin} \frac{n\pi x}{L}$$

$$\frac{\partial^4 y}{\partial x^4} = \sum_{n=0}^{\infty} \frac{n^4\pi^4}{L^4} A_n(t) \operatorname{Sin} \frac{n\pi x}{L} ;$$

Substitute back into equation (1).

$$EI \sum_{n=0}^{\infty} \frac{n^4\pi^4}{L^4} A_n(t) \operatorname{Sin} \frac{n\pi x}{L} = - \rho \sum_{n=0}^{\infty} \ddot{A}_n(t) \operatorname{Sin} \frac{n\pi x}{L}$$

Equating coefficient of sine functions:

$$EI \frac{n^4\pi^4}{L^4} A_n(t) + \rho \ddot{A}_n(t) = 0$$

or,

$$\ddot{A}_n(t) + \left(\frac{1}{\rho} EI \frac{n^4\pi^4}{L^4}\right) A_n(t) = 0$$

This is a wave equation whose frequency is

$$\omega = \sqrt{\frac{EI}{\rho} \frac{n^4\pi^4}{L^4}} = \frac{n^2\pi^2}{L^2} \sqrt{\frac{EI}{\rho}}$$

The solution of the wave equation is:

$$A_n(t) = C_n \operatorname{Sin} \omega t + D_n \operatorname{Cos} \omega t$$

The response frequency is:

$$f = \frac{\omega}{2\pi} = \frac{n^2\pi}{2L^2} \sqrt{\frac{EI}{\rho}}$$

Computer Program

```
C       MAIN
        DIMENSION X(2000),RX(512),GX(512),ID(20),CX(512)
        COMMON T
        COMMON/FT/PX(2,512)
        COMMON/NS/XM(2000)
        DATA R,P/'R','P'/
 1      READ(5,1000) T,KPRT,N,LG,MPLT
C
C       T = DELTA TIME (TIME RESOLUTION IN MSEC).
C       KPRT=0 NO PRINT.
C       KPRT=1 OR MORE, PRINT AUTO-CORRELOGRAM AND POWER SPECTRUM.
C       KPRT=2 PRINT INPUT DATA.
C        MPLT=1 PRINT PLOT EVERY LINE
C        MPLT=0 PRINT PLOT PEAK REGION ONLY
C
 1000 FORMAT (F5.2,7I5)
        IF(N.EQ.0) GO TO 10
        READ (5,1004) ID
 1004 FORMAT (20A4)
        WRITE (6,1015) ID
        FREQNQ=500./T
        DELFQ=1000./LG/T
        WRITE (6,1007) N,LG,KPRT,T,FREQNQ,DELFQ
 1007 FORMAT (/2X'N =',I5,3X'LG(LAG) =',I4,3X'KPRT =',I2,3X'TIME RES.=',F8.4
     *        ,' MSEC',3X'NYQUIST FREQ.=',F10.2,' HZ',3X'FREQ. RES.=',F8.4,
     *         ' HZ'/)
        CALL XDIGIT (X,N)
        IF (KPRT.EQ.2) WRITE (6,1010) (X(I),I=1,N)
 1010 FORMAT (1X20F6.2)
 1015 FORMAT (1H1,1X20A4)
        N2=LG/2
        CALL COVARF (X,LG,N,RX,CX,AVX,SIGX)
        CALL AUTOPS (RX,GX,LG)
        IF (KPRT.GE.1) WRITE (6,1020) ID,AVX,SIGX
        IF (KPRT.GE.1) WRITE (6,1007) N,LG,KPRT,T,FREQNQ,DELFQ
        IF (KPRT.GE.1) CALL TWPLOT (CX,GX,1,N2,-1,R,P,DELFQ)
        GO TO 1
 1020 FORMAT (1H1,1X20A4/10X'AVERAGE =',F12.4,10X,'SIGMA =',F12.4)
 10     CALL RELECE
        END
```

```
      SUBROUTINE AUTOPS (RX,GX,NN)
      DIMENSION RX(NN),GX(NN)
      COMMON/FT/PX(2,512)
      DO 20 K=1,NN
      PX(2,K)=0.
 20   PX(1,K)=RX(K)
      CALL FOUR1(PX,NN,-1)
      DO 30 I=1,NN
 30   GX(I)=PX(1,I)
      RETURN
      END
      SUBROUTINE FOUR1(DATA,NN,JSIGN)                                  FFT10000
      DIMENSION DATA(1)
      N=2*NN                                                           FFT10190
      J=1                                                              FFT10200
      DO 5 I=1,N,2                                                     FFT10210
      IF(I-J)1,2,2                                                     FFT10220
1     TEMPR=DATA(J)                                                    FFT10230
      TEMPI=DATA(J+1)                                                  FFT10240
99    DATA(J)=DATA(I)                                                  FFT10250
      DATA(J+1)=DATA(I+1)                                              FFT10260
      DATA(I)=TEMPR                                                    FFT10270
      DATA(I+1)=TEMPI                                                  FFT10280
2     M=N/2                                                            FFT10290
3     IF(J-M)5,5,4                                                     FFT10300
4     J=J-M                                                            FFT10310
      M=M/2                                                            FFT10320
      IF(M-2)5,3,3                                                     FFT10330
5     J=J+M                                                            FFT10340
      MMAX=2                                                           FFT10350
6     IF(MMAX-N)7,10,10                                                FFT10360
7     ISTEP=2*MMAX                                                     FFT10370
      THETA=6.283185307D0/FLOAT(JSIGN*MMAX)                            FFT10380
      SINTH=SIN(THETA/2.)                                              FFT10390
      WSTPR=-2.*SINTH*SINTH                                            FFT10400
      WSTPI=SIN(THETA)                                                 FFT10410
      WR=1.                                                            FFT10420
      WI=0.                                                            FFT10430
      DO 9 M=1,MMAX,2                                                  FFT10440
      DO 8 I=M,N,ISTEP                                                 FFT10450
      J=I+MMAX                                                         FFT10460
```

```
      TEMPR=WR*DATA(J)-WI*DATA(J+1)                                    FFT10470
      TEMPI=WR*DATA(J+1)+WI*DATA(J)                                    FFT10480
      DATA(J)=DATA(I)-TEMPR                                            FFT10490
      DATA(J+1)=DATA(I+1)-TEMPI                                        FFT10500
      DATA(I)=DATA(I)+TEMPR                                            FFT10510
    8 DATA(I+1)=DATA(I+1)+TEMPI                                        FFT10520
      TEMPR=WR                                                         FFT10530
      WR=WR*WSTPR-WI*WSTPI+WR                                          FFT10540
    9 WI=WI*WSTPR+TEMPR*WSTPI+WI                                       FFT10550
      MMAX=ISTEP                                                       FFT10560
      GO TO 6                                                          FFT10570
   10 RETURN                                                           FFT10580
      END                                                              FFT10590
```

```
      SUBROUTINE COVARF(A,M,N,R,C,AVE,SIGMA)
C     THIS SUBROUTINE CALCULATES AUTOCORRELATION FUNCTIONS FOR DATA SET
C     AM(I), THE ZERO-MEAN DATA REDUCED FROM A(I).   THE SUM OF SQUARES
C     OF A(I) DEVIATED FROM ITS MEAN IS CALCULATED AND ALSO ITS SIGMA.
C     THE AUTOCORRELATION FUNCTIONS, C(I), ARE NORMALIZED BY THE SUM OF
C     SQUARES OF DEVIATIONS AND ARE PLOTTED.  THE UN-NORMALIZED AUTO-
C     CORRELATION FUNCTIONS, R(I), ARE USED TO CALCULATE THE POWER
C     SPECTRAL DENSITY FUNCTIONS.
      DIMENSION A(N),C(M),R(M)
      COMMON/NS/AM(2000)
      SUM=0.
      SS=0.
      DO 10 I=1,N
      X=A(I)
      SS=SS+X*X
 10   SUM=SUM+X
      AVE=SUM/FLOAT(N)
      C0=SS-N*AVE*AVE
      SIGMA=SQRT(C0/(N-1.))
      DO 15 I=1,N
 15   AM(I)=A(I)-AVE
      DO 30 I=1,M
      SUM=0.
      K=N-I+1
      DO 20 J=1,K
      JJ=J+I-1
 20   SUM=SUM+AM(J)*AM(JJ)
      R(I)=SUM/FLOAT(K)
 30   C(I)=R(I)/C0
      RETURN
      END
```

```
      SUBROUTINE TWPLOT (A,B,NI,NF,M,SA,SB,DFQ)
C     THIS IS A 100-COLUMN PRINT PLOT WITH TWO SPECTRA ON THE SAME GRAPH.
      DIMENSION PLOT(101),A(NF),B(NF)
      DATA DOT/'*'/
      DATA PLOT/'+',9*' ','I',9*' ','I',9*' ','I',9*' ',
     1          'I',9*' ','.','.',9*' ','I',9*' ','I',9*' ',
     2          'I',9*' ','I',9*' ','+'/
      AMAX=0.
      BMAX=0.
      L=NI
      DO 10 I=NI,NF
      IF(AMAX-ABS(A(I)))2,2,4
    2 AMAX=ABS(A(I))
    4 IF(BMAX-ABS(B(I)))6,6,10
    6 BMAX=ABS(B(I))
      L=I
   10 CONTINUE
      SCALEA=50./AMAX
      SCALEB=50./BMAX
      WRITE(6,1000) SA,SCALEA,SB,SCALEB,SA,SB
 1000 FORMAT(2(20XA1,' SCALE =',F12.4)/4XA1,6XA1,114X'FREQ'/1X66(2H--))
      DO 20 I=NI,NF
      AA=A(I)*SCALEA
      BB=B(I)*SCALEB
      KA=51.5+AA
      KB=51.5+BB
      KA=MIN0(MAX0(KA,1),101)
      KB=MIN0(MAX0(KB,1),101)
      SAVEA=PLOT(KA)
      SAVEB=PLOT(KB)
      K=I+M
      X=DFQ*FLOAT(K)
      PLOT(KA)=SA
      PLOT(KB)=SB
      IF(KA.EQ.KB) PLOT(KA)=DOT
      IF(MPLT.GT.0.OR.IABS(I-L).LE.10)WRITE(6,2000)AA,BB,K,PLOT,X
      PLOT(KA)=SAVEA
   20 PLOT(KB)=SAVEB
 2000 FORMAT(1XF6.2,1XF6.2,1XI3,1X101A1,F12.3)
      RETURN
      END
```

```
 FORTRANH GO.S
       SUBROUTINE XDIGIT (X,N)
       DIMENSION X(2000)
       COMMON/NS/NSINE(2000)
S60       LI.1        X'F8000'
S         LI.2        X'0005'
S         LI.3        X'0004'
S         LI.4        X'0000'
S         LW.11      *WA(N)
S         WD.2        X'E134'
S10       RD.5        X'E321'
S15       RD.5        X'E321'
S         CW.5        1
S         BCS.3       15S
S         WD.0        X'E135'
S20       RD.6        X'E226'
S         CW.6        3
S         BCS.4       20S
S         RD.10       X'E235'
S         STW.10      NSINE.4
S         AI.4        1
S         BDR.11      10S
       DO30I=1.N
30     X(I)=NSINE(I)/3276.7
       RETURN
       END
```

Unclassified

Security Classification

DOCUMENT CONTROL DATA - R & D

(Security classification of title, body of abstract and indexing annotation must be entered when the overall report is classified)

1. ORIGINATING ACTIVITY (Corporate author)

Industrial Engineering
Louisiana State University
Baton Rouge, Louisiana 70803

2a. REPORT SECURITY CLASSIFICATION

Unclassified

2b. GROUP

3. REPORT TITLE

Data Analysis and Correlation with Digital Computers--Nondestructive Testing

4. DESCRIPTIVE NOTES (Type of report and inclusive dates)

5. AUTHOR(S) (First name, middle initial, last name)

Lawrence Mann, Jr.
Myron H. Young

6. REPORT DATE

September 1, 1971

7a. TOTAL NO. OF PAGES

vi + 75

7b. NO. OF REFS

11

8a. CONTRACT OR GRANT NO.

DAAA 25-69-C0079

b. PROJECT NO.

ARPA Order No. 1246

c.

d.

9a. ORIGINATOR'S REPORT NUMBER(S)

Louisiana State University
Division of Engineering Research
Bulletin No.

9b. OTHER REPORT NO(S) (Any other numbers that may be assigned this report)

10. DISTRIBUTION STATEMENT

Distribution of this document is unlimited.

11. SUPPLEMENTARY NOTES

12. SPONSORING MILITARY ACTIVITY

Advanced Research Projects Agency
Department of Defense
Washington, D. C.

13. ABSTRACT

The purpose of this research was to ascertain feasibility of using digital computers to facilitate nondestructive testing techniques. Energy envelopes were made and were analyzed on the LSU hybrid computer which consists of an EAI 680 for the analog component and a Sigma 5 for the digital component. The sound envelopes were subjected to a filtering program making use of the Fourier analysis in order to arrive at a response frequency. The response frequency for "good" specimens were compared against the response frequency for faulty specimens.

During the course of the investigations nondestructive tests were investigated which included stress analysis, dimensional properties, faulty specimens and faults in long, thin wall tubing.

The conclusions reach from these investigations showed that it was entirely feasible to automate nondestructive testing techniques using energy envelope media. Applications of this technique in the fields of machine components inspection, casting inspection, fabricated rolled steel, and airframes appears to offer promise.

DD FORM 1 NOV 1473 REPLACES DD FORM 1473, 1 JAN 64, WHICH IS OBSOLETE FOR ARMY USE.

Unclassified

Security Classification

14. KEY WORDS	LINK A		LINK B		LINK C	
	ROLE	WT	ROLE	WT	ROLE	WT
Non-Destructive Testing Computer Analysis Acoustical Analysis						